Topical reinforcement of the cervical mucus barrier to sperm

Authors: Ulrike Schimpf[1, 2Ψ]*, Erika Caldas-Silveira[3Ψ], Ljudmila Katchan[4], Cécile Vigier-Carriere[4], Isabelle Lantier[5], Gilai Nachmann[1], Sebastian Gidlöf[6,7], Aino Fianu Jonasson[6,7], Lars Björndahl[8], Stéphane Trombotto[9], Xavier Druart[3], Thomas Crouzier[1,4,10,11]*

Affiliations:
[1]Division of Glycoscience, Department of Chemistry, School of Engineering Science in Chemistry, Biotechnology and Health (CBH), AlbaNova University Center, KTH Royal Institute of Technology, 106 91 Stockholm, Sweden
[2]Department of Material and Environmental Chemistry (MMK), Stockholm University, 106 91 Stockholm, Sweden
[3]PIXANIM, Physiologie de la Reproduction et des Comportements, UMR INRAE, CNRS, Université de Tours, IFCE, 37380 Nouzilly, France
[4]Cirqle Biomedical Contraception ApS, Ole Maaløes Vej 3, 2200 Copenhagen, Denmark
[5]French National Institute for Agriculture, Food, and Environment (INRAE), UMR ISP, Université de Tours, 37380 Nouzilly, France
[6]Department of Gynecology and Reproductive Medicine, Karolinska University Hospital, 141 86 Stockholm, Sweden
[7]Department of Clinical Science, Intervention and Technology (CLINTEC), Karolinska Institutet, Alfred Nobels alle 8, 141 52 Huddinge, Sweden
[8]ANOVA - Andrology, Sexual Medicine, Transmedicine, Karolinska University Hospital and Karolinska Institutet, Norra Stationsgatan 69, 113 64 Stockholm, Sweden
[9]Ingénierie des Matériaux Polymères (IMP), CNRS UMR 5223, Université Claude Bernard Lyon 1, 69622 Villeurbanne, France
[10]AIMES - Center for the Advancement of Integrated Medical and Engineering Sciences at Karolinska Institutet and KTH Royal Institute of Technology, 171 77 Stockholm, Sweden
[11]Department of Neuroscience, Karolinska Institutet, 171 77 Stockholm, Sweden

[Ψ]Co-first authorship
*Corresponding author:
Thomas Crouzier: crouzier@kth.se
Ulrike Schimpf: schimpf@kth.se

Abstract

Close to half of the world's pregnancies are still unplanned, reflecting a clear unmet need in contraception. Ideally, a contraceptive would provide the high efficacy of hormonal treatments, without the systemic side effects of hormones. Here we propose topical reinforcement of the cervical mucus by chitosan mucoadhesive polymers as a form of female contraceptive. Chitosans larger than 7 kDa effectively crosslinked human ovulatory cervical mucus to prevent sperm penetration in vitro. We then demonstrated in vivo using the ewe as a model that vaginal gels containing chitosan could stop ram sperm at the entrance of the cervical canal and prevent them from reaching the uterus, whereas the same gels without chitosan did not significantly limit sperm migration. The chitosan did not affect sperm motility in vitro or in vivo, suggesting reinforcement of the mucus physical barrier as the primary mechanism of action. The chitosan formulations did not damage or irritate the ewe vaginal epithelium, in contrast to nonoxynol-9 spermicide. The demonstration that cervical mucus can be reinforced topically to create an effective barrier to sperm may therefore form the technological basis for muco-cervical barrier contraceptives with the potential to become an alternative to hormonal contraceptives.

Introduction

Family planning promotes education, reduces gender inequalities, improves child and maternal health, and by doing so decreases poverty and hunger *(1)*. In some regions such as the US and EU, access to effective female contraceptives beginning in the 1960s with the advent of hormonal birth control has facilitated family planning and contributed to increased equality between men and women *(2, 3)*. However, 40% of pregnancies globally are still unintended *(4),* mainly due to the lack of contraceptives use. In the US, 47% of women have discontinued a contraceptive due to side effects *(5)*, highlighting the need for new reliable and more desirable contraceptive options *(6)*. Ongoing efforts to create long-acting contraceptives and male contraceptives will address part of the need for contraception. Another part can be addressed by creating contraceptives with user-preference in mind to ensure maximum compliance. In particular, several studies have shown that there is a large interest for "on demand" contraceptives which prevent pregnancy at or around the time of intercourse. For instance, Foster et al. showed that 70% of women in abortion clinicals and over 50% of women in family planning clinics were interested in a hypothetical pericoital contraception pill *(7, 8)*.

Although hormonal contraception offers high efficacy rates, a substantial proportion of users express a non-hormonal preference for their contraceptive *(9)* or discontinue their use, driven in large part by their perceived risks of side effects *(10)*. Existing non-hormonal alternatives are hampered by lack of efficacy or side effects and result in high discontinuation rates. In clinical trials, the 1-year discontinuation rate was at 49% for diaphragm with spermicides *(11)*, and above 50% for nonoxynol-9 spermicides *(12, 13)*. Even long-acting copper intrauterine devices (IUDs) suffer a 20% discontinuation rate, in part due to dislocation and pain *(14, 15)*. Condoms and spermicides are less invasive than copper IUDs but are also much less effective in typical use than hormonal methods *(13, 16)*. The withdrawal of the US pharmaceutical industry from contraceptive research and development since the 1980 has led to only minor improvements of existing methods, and has comforted our dependence on 19th and 20th century approaches to birth control *(17)*. There is thus a clear need for alternative mechanisms of action for female contraceptives.

Cervical mucus (CM) is a gel secreted in the cervical canal isolating the bacteria-rich vagina from the uterus and the upper reproductive tract. It is mainly composed of high molecular weight mucin glycoproteins, which adopt an extended linear conformation and interact to form a hydrated network. The mucins interact with other globular proteins, lipids and salts that define the physical, mechanical, and biological properties of CM. In the time leading up to ovulation, high serum estradiol concentrations drive changes in rheological properties, microstructure, and chemical composition of the CM, which allow the CM to transition to a selective barrier, allowing the passage of a few thousand sperm down from tens or hundreds of millions of a typical ejaculate *(18, 19)*. The cervix and its mucus thus act as regulators of sperm transport in the female reproductive tract, and reinforcement of the CM to block sperm passage has been proposed as a possible contraceptive strategy *(20)*. For instance, progestin-only pills and levonorgestrel intrauterine systems act, at least in part, by thickening the CM *(20)*. However, the successful reinforcement of CM through a non-hormonal method, topical or systemic, has remained elusive *(21–24)*.

Mucus engineering approaches to alter the mucus gel properties via topical treatments are emerging as promising approaches to address mucus-related conditions such as mucosal dryness *(25)*, infections, inflammation *(26)*, and microbiome dysbiosis *(27)*. However, they lack thorough in vivo validation and have not been successfully applied to contraception. In this work, we developed a non-hormonal approach

to reinforce the CM barrier to sperm by physically crosslinking the mucin network of the mucus gel. We used chitosan (CS), a biopolymer of β-linked D-glucosamine and N-acetyl-D-glucosamine, obtained by the deacetylation of chitin extracted from fungal cell wall or crustacean shell. Chitosan has been extensively studied in biomedical applications, in particular because of its mucoadhesive properties *(28)*. We have previously shown that chitosan polysaccharides could crosslink porcine gastric mucin gels, thereby reinforcing its barrier properties *(29)*. We here demonstrated that chitosan can crosslink ovulatory CM and by doing so can impair sperm penetration both in vitro using human ovulatory CM and in vivo in the ewe without evidence of cytotoxicity towards vaginal epithelial tissues and sperm. This work suggests the feasibility of a novel mucus-centric mechanism of action for a female contraceptive.

Results

Chitosan diffuses into human cervical mucus

We first investigated the ability of chitosans dissolved in low concentration of lactic acid (32.5 mM, pH 5.5) to penetrate human ovulatory CM. The low pH of the lactic acid solution used to dissolve chitosan is necessary to ensure the chitosan is soluble when exposed to the vagina and then to the cervical canal (**Fig. S1)**; chitosan typically precipitates above pH 6 *(30)*. In addition to lactic acid, we also tested the addition of a thickening agent to the chitosan formulation. Hydroxyethyl cellulose (HEC) is commonly used in placebo vaginal formulations applied in clinical trials of vaginal products *(31)*. Thickening agents such as HEC are used in vaginal formulations to increase the residency time of the chitosans in the vagina to optimize the gel's spreading and coverage of the cervix, while preventing leakage of the formulation. Transmittance measurements of the HEC formulation were not affected by the addition of chitosan, suggesting that HEC and chitosan do not strongly interact, and that HEC is an appropriate excipient (**Fig. S1**).

We let chitosan passively diffuse into CM rather than actively mixing the two components to mimic a topical treatment of the mucus. This was conducted by exposing one side of the CM-filled capillary to the chitosan solution and letting the chitosan diffuse into the CM (**Fig. 1A**). All chitosans accumulated at the interface of the CM gel but also diffused within the gel, forming a concentration gradient (**Fig. 1, B to E**). After 30 minutes of diffusion, we analyzed the concentration gradient that formed through the capillary (**Fig. S2**). The maximum penetration distance of the chitosans was dependent on the molar mass of the chitosan (**Fig. 1, F to I**), with detection at 3.5 mm into the mucus for 1.4 kDa chitosan versus only 1.5 mm for the 150 kDa chitosan tested. The diffusion coefficients calculated from the penetration distances showed an 11-fold difference between the more diffusive 1.4 kDa chitosan oligomer and the less diffusive 150 kDa chitosan (**Fig. 1J**). Faster diffusion of the smaller chitosans also led to more chitosan accumulation into the ovulatory CM, with the calculated area under the curve being 15 times larger for the 1.4 kDa chitosan than for the 150 kDa chitosan (**Fig. 1K**). We also found the presence of HEC did not affect maximum diffusion distance, chitosan diffusion coefficient, or accumulation (**Fig. 1, I to K**).

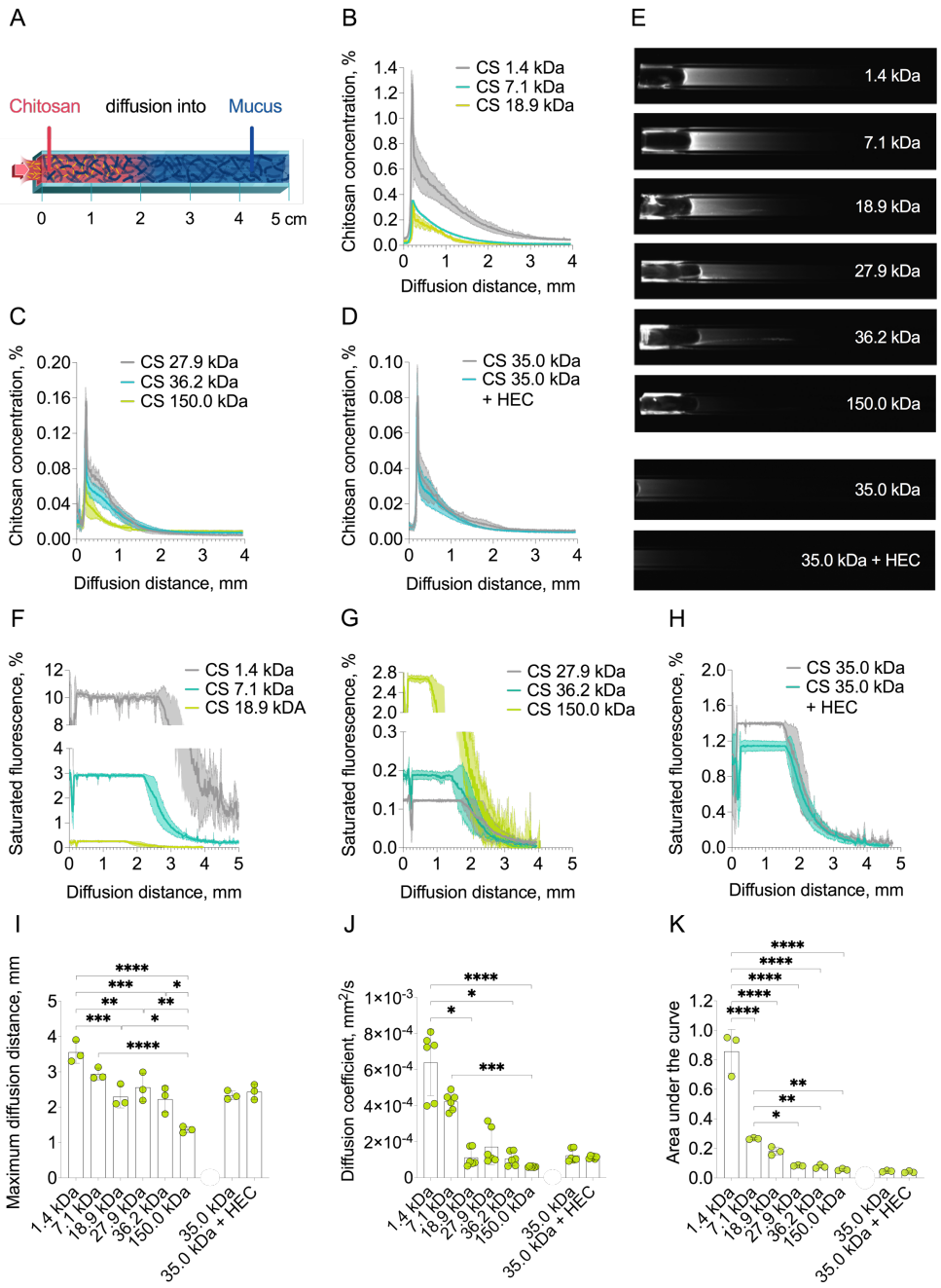

Figure 1. Diffusion of oligo- and polymeric chitosans into human ovulatory cervical mucus. A) Square capillaries filled with human cervical mucus (CM) are exposed to solutions of fluorescently labeled chitosan with or without hydroxyethyl cellulose (HEC) to evaluate the ability of chitosan to interact and diffuse into the mucus. **B** to **D**) Overview of the CHITOSAN distribution over the length of the capillary, highlighting chitosan accumulation at the CM gel interface. **E**) Representative images of ovulatory CM-filled capillaries after exposure to CHITOSAN solutions for 30 min at 20 milliseconds (ms). **F** to **H**) Chitosan distribution profiles obtained from over-exposed images (800 ms) revealing the diffusion fronts of the CHITOSAN into the mucus. Each curve is the mean of three replicates and the colored area represents the standard deviation. The measurements were conducted with CM collected from one or more donors. **I**) The maximum diffusion distance, and **J**) the diffusion coefficient for CHITOSAN in CM calculated as described in the supplementary materials and methods section of the supplementary information. **K**) Relative total amounts of CHITOSAN accumulated in the CM as measured by the area under the CHITOSAN distribution profile

curve. The graphs I to K show individual values from independent experiments, their mean values, and the standard deviation. Normality was tested using the Shapiro-Wilk test. Statistical differences between groups were tested via Tukey's test or Dunn's test for the Area area under the curve and Maximum maximum diffusion distance or the diffusion coefficient. Asterisks denote statistically significant increases or decreases (*pP<0.05, **pP<0.01, ***pP<0.001, ****pP<0.0001).

Chitosan reinforces the barrier properties of human ovulatory cervical mucus

We then asked if exposing chitosans to human ovulatory CM could affect the ability of sperm to penetrate and swim through the mucus. We used a sperm penetration assay, in which we first exposed a chitosan solution to the opening of a square capillary filled with ovulatory CM (**Fig. 2A**). We then replaced the chitosan with a solution of fresh undiluted semen and assessed sperm penetration. We selected the fertile phase of CM with a "good" or "excellent" Insler score *(32)*, and selected high-quality semen used within minutes of collections (**Tables S1 and S2**).

Pre-treatment of the ovulatory CM with 1.4 kDa chitosan allowed sperm to penetrate the whole length of the capillary (**Fig. 2B**). However, treatments with chitosans larger than 7.1 kDa limited the maximum penetration distance, defined as the distance at which there is less than 10 cumulative sperm present in the three fields of view analyzed (**Fig. 2B**). Robust decreases in sperm numbers compared to treatment with lactic acid solution only were observed with chitosans larger than 18.9 kDa. Exposure of CM to lactic acid also lowered sperm numbers, possibly due to residual lactic acid in the mucus, or to structural changes caused by transient acidification (**Fig. 2, C to K**). The addition of HEC to the formulation did not alter the effectiveness of the 35 kDa chitosan (**Fig. 2, J and K**). Close to the CM-semen interface (0.1 mm into the gel phase) treating the CM with lactic acid solution without chitosan allowed more sperm into the mucus gel, likely owing to a slight dilution of the mucus (**Fig. 2L**). All chitosan treatments except 1.4 kDa chitosan markedly reduced the sperm count compared to the control CM (**Fig. 2L**).

Mixing short oligo-chitosans with larger chitosans inhibited the barrier reinforcing effect (**Fig. S3**), likely because short chitosans diffused in the CM faster than larger chitosans, blocking binding sites for the larger chitosans. The 36.2 and 35 kDa chitosans struck a balance between reproducible barrier reinforcement and diffusion into CM. We thus selected a 36.2 kDa fungal-derived chitosan for further studies because the animal-free formulation could facilitate further technological development. This chitosan was also able to rapidly reinforce the human CM barrier to sperm, with a reduction in sperm penetration after 1 minute of exposure and full sperm blockage after 5 minutes (**Fig. S4**), enabling the possibility of rapid onset of action.

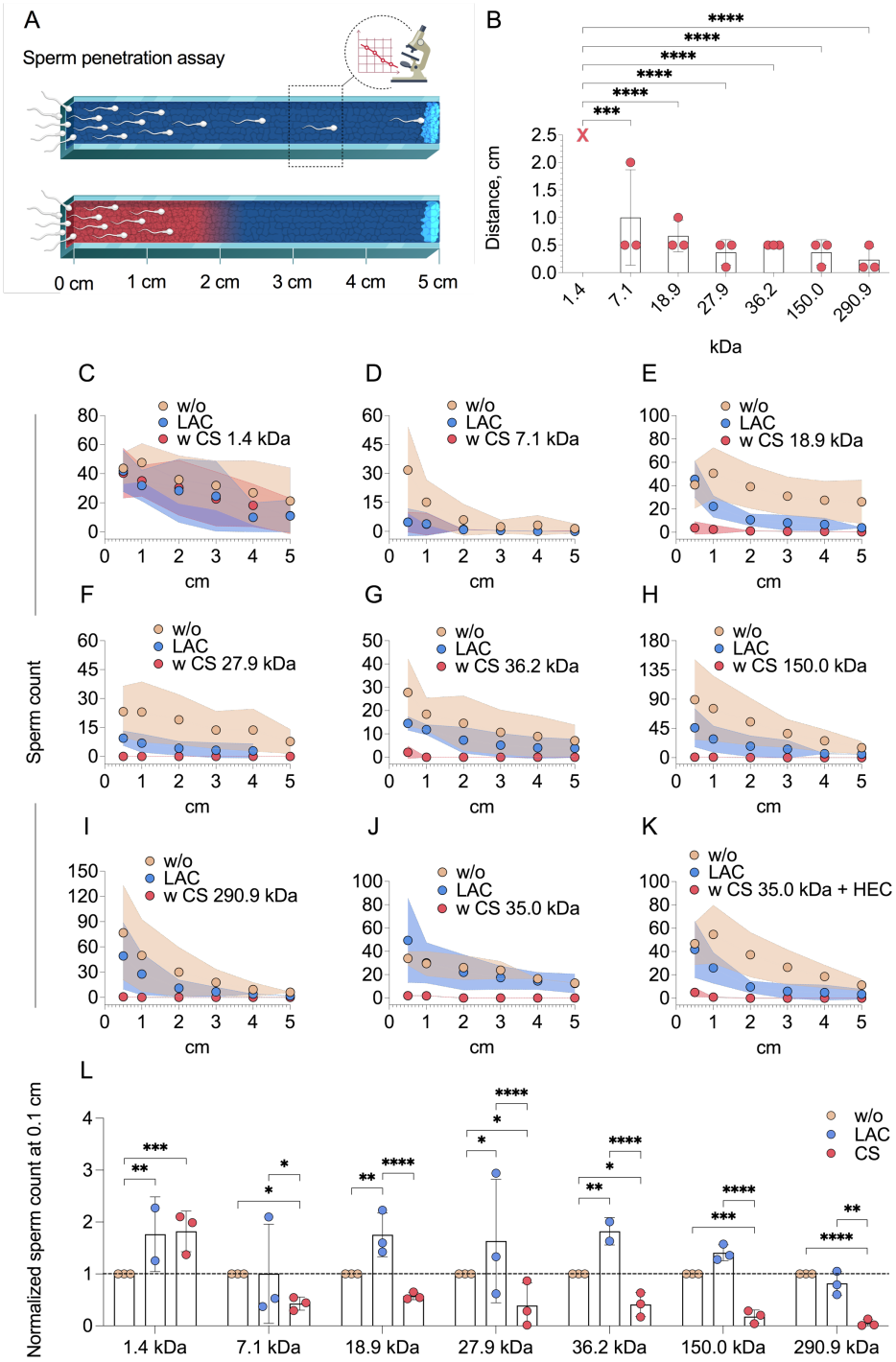

Figure 2. Penetration of sperm through human ovulatory cervical mucus. **A**) The sperm penetration assay consists consisted in of counting sperm through the length of a 5 cm capillary filled with treated or untreated CM after 30 minutes of exposure to semen. **B**) The maximum penetration distance is shown, defined as the distance at which less than 10 cumulative sperm were detected in the three fields of view analyzed. The graph represents individual values, their mean values and the standard deviation. **C** to **K**) Sperm counts through capillaries treated with chitosans solutions of varying molar masses with and without hydroxyethylcellulose (HEC), showing mean values and standard deviations. Each point is the mean of three replicates and the colored area represents the standard deviation. **L**) Sperm counts normalized to CM without treatment (w/o), for lactic acid- treated CM (LAC) and for treatment with various

chitosans of different molar masses (CS), 0.1 cm inside the CM, close to the semen/CM interface. Each measurement was conducted in triplicate, using one or more CM samples and semen of from at least two donors. Replicates are the mean of the sperm count at three different fields at each distance. The graph represents the nine resulting values, their mean values, and the standard deviation. Statistical differences between groups were tested using the D'Agostino and Pearson test followed by Tukey's test. Asterisks denote significant increases or decreases (*pP<0.05, **pP<0.01, ***pP<0.001, ****pP<0.0001).

Chitosan treatment reinforces the cervical mucus barrier in the ewe model

Although the sperm penetration assays validated the feasibility of forming a barrier resistant to sperm penetration on human ovulatory cervical mucus, they did not take into account the challenge of delivering the chitosan, the contractions, movements, and resulting shear on the formulation and mucus during intercourse, and the dynamic mucus turnover that this approach would face in humans. Thus, we tested whether a chitosan formulation could reinforce the barrier to sperm in vivo, using the ewe as a model **(Fig. 3, A and B)**.

We first tested whether chitosan could reinforce the barrier properties of ovulatory CM collected from ovulating ewes in a sperm penetration assay using ram sperm. Two chitosans that we found to be effective on human ovulatory CM were also effective on the ewe ovulatory CM, albeit with higher sperm counts at the entrance of the capillary (**Fig. S5 and Table S3**). We attributed this difference to the low viscosity of the ewe ovulatory CM because it was mixed with vagina secretions during collection. We tracked the distribution of the formulation in the ewe's reproductive tract using chitosan labeled with the Atto-665 fluorescent dye. We detected high fluorescence emission in the vagina at the moment of artificial insemination using probe confocal laser endoscopy (pCLE), 1 h after gel administration (**Fig. 3C)**. Then, 4 h after artificial insemination (5 h after gel administration), fluorescence measurement of explanted tract showed that the chitosan spread throughout the vagina and penetrated up to 2 cm into the cervix, corresponding to where the first cervical ring is *(33)* (**Fig. 3, D and E, and Fig. S6**).

The formation of a barrier to sperm was then assessed by localizing with pCLE the sperm throughout the reproductive tract. As expected, we found large numbers of highly motile sperm in the vagina immediately after artificial insemination (AI) (**Fig. 3F**). In untreated ewes (n=13) or ewes treated with HEC gel only (n=7), sperm effectively migrated up the reproductive tract. We found high numbers in the vagina and at the entrance of the cervix and lower numbers in the distal part of the cervix and in the uterus. In sharp contrast, we measured a marked reduction in the number of sperms in the distal cervix and in the uterus in chitosan-treated ewes (n=8, **Fig. 3G**). Out of the 8 animals in the chitosan-treated group, only one had 2 sperm detected in the uterus (see raw data **Table S4**), corresponding to a 98% decrease in average uterine sperm numbers compared to the untreated control animals. This effect is partially attributed to the HEC and lactic acid excipients, which can account for 44% decrease in sperm number.

These results suggested that an effective barrier to sperm was formed in the cervical canal between the cervical os and the uterus, preventing sperm migration within this 4-hour time frame. Indeed, 4 hours after AI, the sperm in the vagina of untreated, HEC only, or HEC with chitosan treated ewes still showed a high rate of motility compared to immediately after AI (**Fig. 4, A and B**). This is in part because the ewe vagina has a pH that is close to neutral *(34)* (**Fig. S7**), which is in contrast to the human vagina, in which the acidic pH *(35)* and immune response immobilize sperm within hours *(36)*. The HEC gel alone was not sufficient

to form an effective barrier in the ewe, although a small reduction in sperm numbers was seen, probably due to the physical barrier the HEC gel creates. The lactic acid content of the HEC gels did not have the effect seen in the in vitro sperm penetration assays (**Fig. 2, C to K**), likely because the ratio of lactic acid to mucus in vivo was much smaller than in vitro in which 100 µL was exposed to 4 µL of mucus.

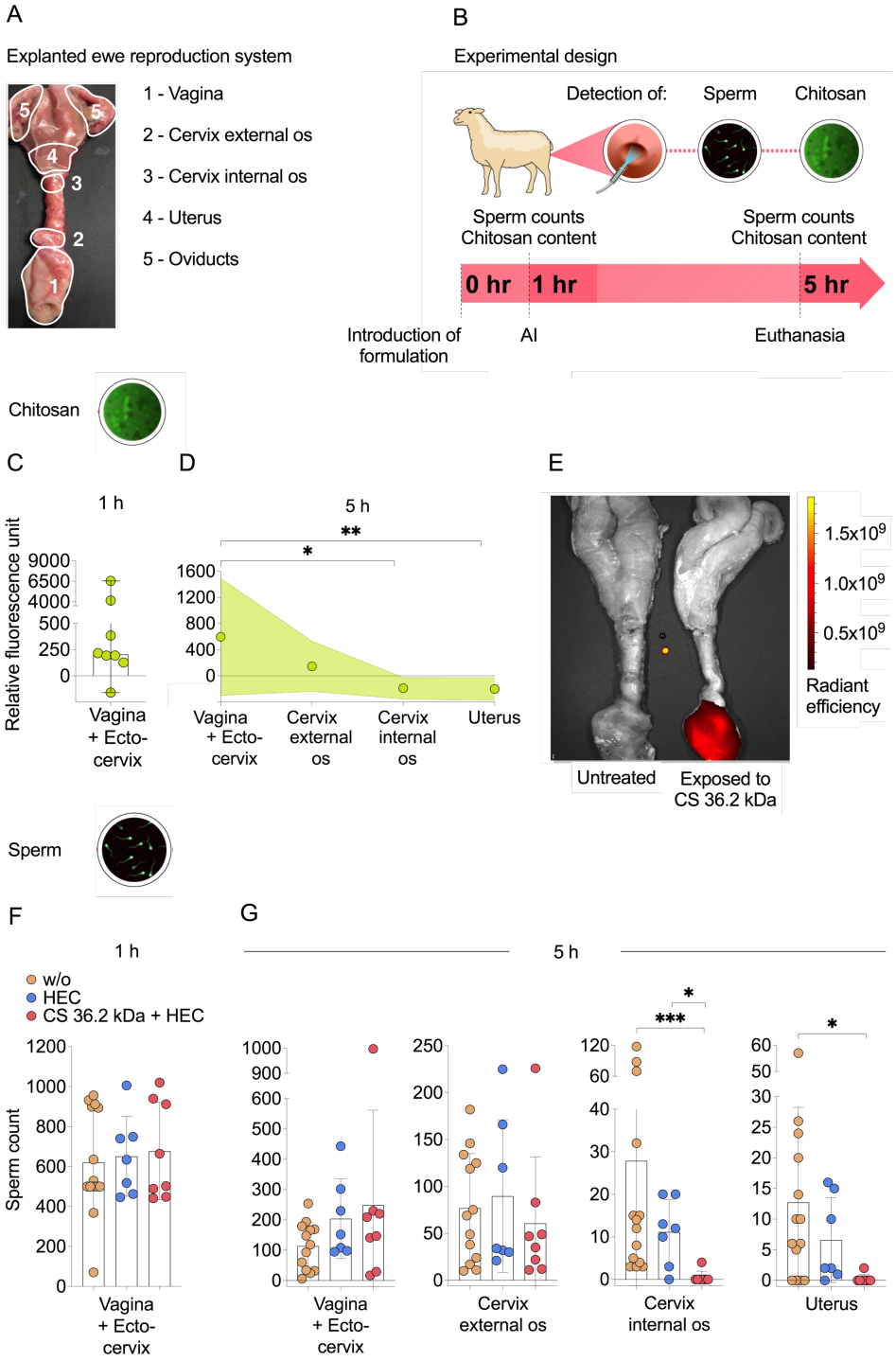

Figure 3. Formulation delivery and sperm migration through the ewe reproductive tract. A) Picture of the after 5 h explanted ewe reproduction system. Subdivision of the ewe reproductive tract to study the diffusion of chitosan and sperm penetration in vivo after insemination: Vagina (1), Cervix external (2) and internal (3) orifice (os), Uterus

(4) and Oviducts (5). **B**) Experimental design: The experiments consisted in treating ovulating ewes were treated with hydroxyethyl cellulose (HEC) in lactic acid, or chitosan and HEC (CS 36.2 kDa + HEC) in lactic acid, followed by artificial insemination (AI) one hour later. The sperm numbers throughout the reproductive tract were counted, and the localization of chitosan determined by probe confocal laser endoscopy (pCLE) imaging. **C**) Chitosan distribution in the ewe reproductive tract as measured by pCLE immediately after artificial insemination (1 h after administration), n=8. The graph represents individual values, their mean values, and the standard deviation. **D**) Chitosan detection by pCLE measurement along the reproductive tract of the ewe 5 h after gel administration. Each point is the mean of eight biological replicates and the colored area represents the standard deviation. Statistical references between groups were tested via the Shapiro-Wilk test followed by the Dunn's test. **E**) IVIS sSpectrum image of ewe reproductive tract without treatment (left), and 5 h after chitosan gel administration (right), revealing the localization of chitosan. **F**) Sperm counts derived from the image analysis of pCLE videos taken in the vaginal cavity immediately after artificial insemination (1 h post after gel administration), and **G**) throughout the reproductive tract four hours later (5 h post after gel administration). HEC only and CS 36.2 kDa + HEC conditions were tested on n=7 and n=8 ewes, respectively, and untreated control ewe (w/o) on n=13 ewes. The graphs represent individual values of independent biological samples, their mean values and the standard deviation. Statistical references between groups were tested via the Shapiro-Wilk test followed by the Dunn's test. Asterisks denote significant increases or decreases (*pP<0.05, **pP<0.01, ***pP<0.001).

Chitosan barrier reinforcement is not mediated by spermicidal action

In addition to the direct effects of chitosan on cervical mucus, the chitosan formulation could interfere with sperm migration by affecting viability and motility. We have previously shown that oligo-chitosans are relatively inert towards human sperm *(37)*, however, these differ in molar mass to the chitosan used herein. In the ewe, the proportion of motile sperm in the vagina and ecto-cervix was near 100% immediately after AI, even in the presence of HEC and HEC/chitosan formulations **(Fig. 4A)**. In the vagina and at the cervical entrance, the proportion of motile sperm remained unaffected compared to control, even after thorough spreading and mixing of the formulation had occurred 4 hours after AI due to the ewe's movements **(Fig. 4B)**. Deeper in the reproductive tract, at the internal cervix and uterus, the number of sperms were too low to assess motility. However, in the external os, sperm were present but with decreased motility likely due to the presence of crosslinked mucus, which immobilized a fraction of the sperm. The same phenomenon was observed in the in vitro sperm penetration assay in which spermatozoa were immobilized by the chitosan-complexed mucus but still actively beating their flagella (**Movie S1 and S2**).

For a more quantitative assessment of the direct effect of chitosan on sperm motility, and on their ability to penetrate CM, we exposed human sperm to HEC (pH 5.5) with or without chitosans and measured the impact on sperm kinematic parameters by Computer Aided Sperm Analysis (CASA). The chitosan formulation did not affect the kinematic parameter motility and velocity of human sperm compared to HEC gels only **(Fig. 4, C and D)**. Although the kinematic values of sperm decreased over time due to the presence of seminal fluid *(38)* and the acidity of the HEC gels *(39)*, the chitosan did not have any additional effect (**Fig. S8**). A direct effect of chitosan on sperm motility was thus considered unlikely to be the main contributor to the barrier. Because HEC formulations alone were poorly effective at blocking sperm in vivo (**Fig. 3G**), we concluded that the blockage of sperm transport to the distal cervix and uterus by the chitosan treatment in the ewe was mediated by chitosan and its physical alteration of the CM barrier.

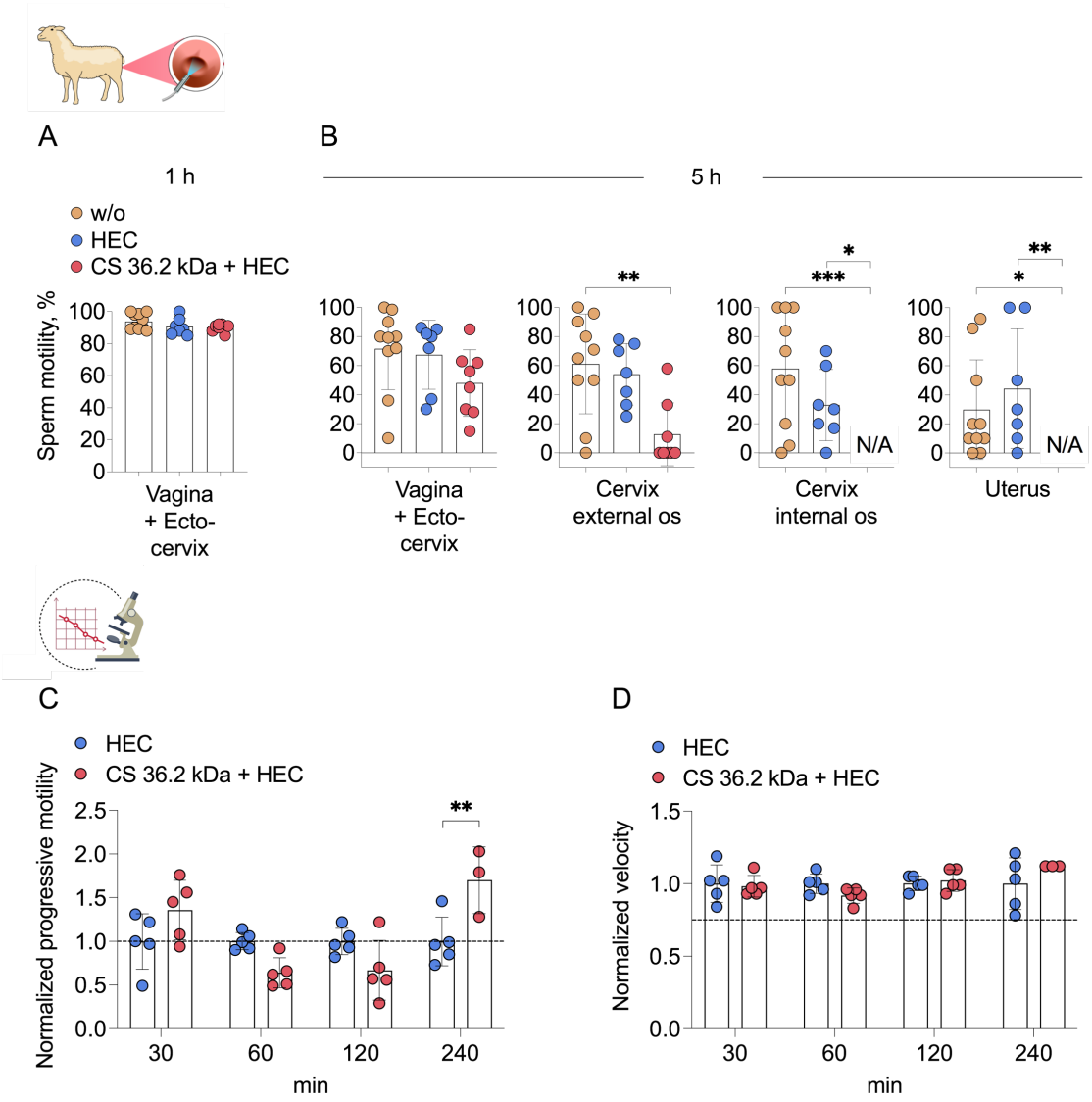

Figure 4. Effect of chitosan on ram and human sperm kinematic motility and velocity. A) Proportion of motile sperm in the vaginal cavity of the ewe with no treatment (w/o, *n*=10), with HEC only (*n*=7), and with chitosan in a HEC gel (CS 36.2 kDa + HEC, *n*=8) immediately after artificial insemination (1 h post after administration of formulation), and **B**) throughout the ewe's reproductive tract 4 hours post artificial insemination (5 h post after administration of formulation). The graphs represent individual values of independent biological samples, their mean values, and the standard deviation. Statistical differences between groups were tested using the Kolmogorov-Smirnov test followed by Dunn's test. **C**) Progressive motility and **D**) velocity of human sperm exposed to chitosan containing gels (CS 36.2 kDa + HEC, *n*=5) measured in vitro by CASA and normalized to motility and velocity of human sperm exposed to the gel without the chitosan (HEC, *n*=5). A semen sample containing sperm that exhibits high progressive motility (mean 88%) was used. The graphs represent individual values of technical replicates, their mean values, and the standard deviation. Statistical differences between groups are tested via the D'Agostino and Pearson test followed by the Sidak's test. Asterisks denote significant increases or decreases (*pP<0.05, **pP<0.01, ***pP<0.001).

Chitosan formulations are non-cytotoxic, induce low concentrations of inflammatory cytokines, and do not alter vaginal epithelial thickness

Spermicides have a history of vaginal epithelial irritation leading to discomfort, and possible increased risks of infections *(40)*. Decades of chitosan research have shown that chitosan-based materials are generally biocompatible with a range of implantation sites *(41)*. This is further validated by the successful approval in the USA and in the EU of several medical devices including chitosans such as hemostatic materials *(42–44)* (e.g., HemCon®, Syvek®, Clo-Sur®, ChitoSeal®), nerve guides *(45)* (NeuroShield™) and in carboxymethylated versions as injections to treat osteoarthritis of the knee *(46)* (KioMedine^{vs}one). However, the biocompatibility profile of chitosan is dependent on its molecular features, including molar mass, deacetylation degree (DDA), and impurities, and it could be tissue dependent.

To assess the risk of the chitosan formulation to vaginal tissues, we first tested for epithelial irritation by exposing three-dimensional vaginal epithelial tissue to the HEC/chitosan formulation. The chitosan was restricted to the upper layer of the cells of the tissue, which suggests the treatment was localized and that chitosan was unlikely to be absorbed systemically (**Fig. 5A**). The cells of the tissue model maintained cell viability after 24 hours exposure to chitosan formulation. In contrast, nonoxynol-9 (N9) spermicide, which is known to irritate vaginal tissues, led to a 91% reduction in cell viability compared to the untreated tissues after 24 hours' exposure (**Fig. 5B**). In addition to cell viability, pro-inflammatory cytokine secretion, in particular IL-1α, is a risk factor for vaginal irritation by topical formulations *(47)*. We measured a dose-dependent but limited increase in IL-1α cytokine release from tissues exposed to the formulation containing chitosan compared to those exposed to HEC gels, whereas N9 formulation led to release 12 times higher than no treatment control baseline (**Fig. 5C**).

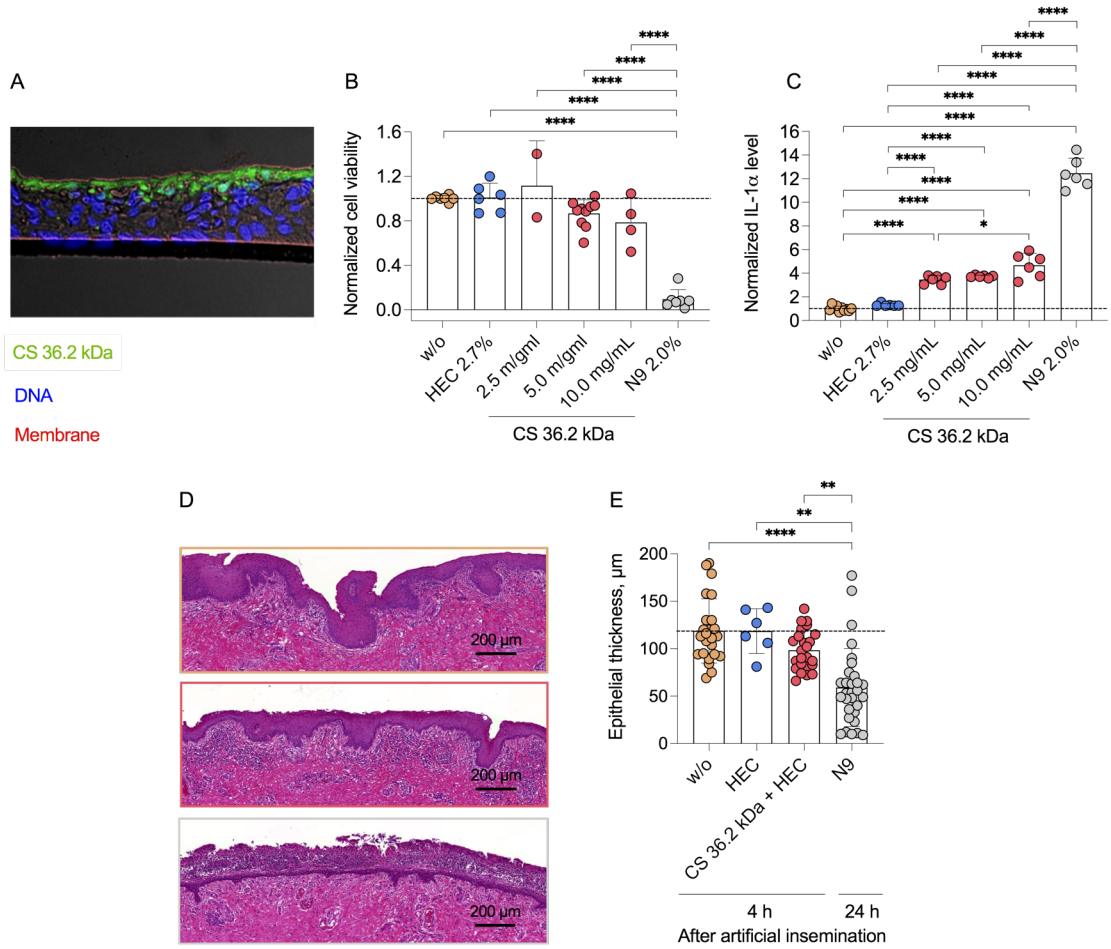

Figure 5. Cytotoxic assessment of chitosan. A) Distribution of chitosan labeled with fluorescein isothiocyanate (FITC) in a 3-dimensional vaginal epithelial model after a 24-hour exposure. **B**) Cytotoxicity after 24 hours exposure to hydroxyethyl cellulose (HEC) gel (*n*=6), HEC gels with chitosan at concentrations of 2.5 (*n*=2), 5 (*n*=10), and 10 mg/mL (*n*=4), and the nonoxynol-9 (N9) spermicide (*n*=7), compared to untreated tissue (w/o, *n*=7). **C**) Concentration of the inflammatory marker IL-1α after a 24-hour exposure to HEC gel (*n*=6), HEC gels with chitosan at concentrations of 2.5 (*n*=6), 5 (*n*=6), and 10 mg/mL (*n*=6), and the nonoxynol-9 (N9) spermicide (*n*=6) in comparison with untreated cells tissue (*n*=10). **D**) Histological cross-section of ewe vaginal epithelium stained with eosin and hematoxylin with the control on the top, the epithelium exposed for 4 hours to HEC gels with 5 mg/mL chitosan in the middle and exposed for 24 hours to the nonoxynol-9 (N9) spermicide in the bottom. The length of the scale bar corresponds to 200 µm. **E**) Quantification of epithelial thicknesses for non-exposed (w/o, 4 hours, *n*=24, four ewes) ewe vaginal epithelium and epithelium exposed to HEC (4 hours, *n*=6, one ewe), HEC gels with 5 mg/mL chitosan (4 hours, *n*=24, four ewes) and nonoxynol-9 (N9) spermicide (N9, 24 hours, *n*=30, five ewe). The graphs represent individual values of independent biological samples, their mean values, and the standard deviation. Statistical differences in cell viability and Il-1a concentration between the control (w/o) and treated samples were tested using the Shapiro-Wilk test followed by the Tukey's test. To test for significant differences in epithelial thickness between groups, we used the Shapiro-Wilk test followed by the Dunn's test. Asterisks denote significant increases or decreases (*pP<0.05, **pP<0.01, ****pP<0.0001).

To test the effect of the treatment in vivo, vaginal epithelial tissue from the efficacy studies **(Fig. 3**) were collected after the 5-hour exposure. In contrast to the N9 treatment that led to shedding of the epithelium, the HEC gel with chitosan showed no effect compared to HEC alone (**Fig. 5, D and E**). In addition, a

histopathological scoring of the histology slides showed no effect of the chitosan treatment compared to untreated animals, and increased inflammation and atrophy scores in the N9 treated animals (**Table 1)**.

Table 1. Histopathological analysis of vaginal biopsies. Mucosal epithelium was screened for irritation and inflammation using untreated tissues (Untreated), tissues treated with chitosan of 36.2 kDa (CS 36.2 kDa) and hydroxyethyl cellulose (HEC), and the spermicide nonoxynol (N9). Biopsies were analyzed for 6 (Untreated), 4 (CS 36.2 kDa) and 5 (N9) ewes (E).

		Untreated						CS 36.2 kDa + HEC				N9				
		E1	E2	E3	E4	E5	E6	E1	E2	E3	E4	E1	E2	E3	E4	E5
Sub-mucosa	Mononuclear cells[#]	2	2	2	2	2	2	2	2	1	2	1	0	1	0	0
	Acute hemorrhage	0	0	1	1	1	1	0	0	0	0	0	0	0	0	0
Epithelium	Neutrophilic cells[#]	2	1	1	1	2	1	2	1	0	1	0	0	0	0	0
	Erosion	1	0	0	0	1	1	1	0	0	0	0	**4**[a]	0	2	0
	Neutrophilic microabscess	1	0	1	0	1	1	1	0	0	0	0	0	0	0	1
	Hypertrophy	1	0	1	0	2	1	0	1	0	1	0	0	2	0	0
	Squamous metaplasia	0	1	0	0	1	1	1	2	0	1	0	0	1	1	1
	Mucoid cellular shedding	0	1	0	0	0	1	1	1	1	1	0	0	0	0	0
	Apoptosis	0	0	1	1	2	0	0	1	0	0	0	0	0	2	0
	Inflammation	0	0	0	0	0	0	0	0	0	0	**3**[b]	**3**[c]	0	1	1
	Atrophy	0	0	0	0	0	0	0	0	0	0	2	**4**	0	0	0

[#]Infiltration, [a]With evidence of ulceration, [b]Acute, large crust formation, [c]Acute/subacute, extending into the dermis with neovascularization.

Discussion

In this work, we hypothesized that the interaction of the mucoadhesive chitosan biopolymer with CM could create an impenetrable barrier to sperm. We first sought to study the interaction of the chitosans varying in molar mass, with human ovulatory CM. We observed accumulation of all chitosans at the interface of the gel, likely resulting from the strong interactions between chitosan and the CM (**Fig. 1, B to E**). Several other mucoadhesive polymers and peptides have also been shown to accumulate at the interface of mucin gels *(48–50)*. The superior diffusion profile and accumulation of smaller chitosans was likely due to limited steric hindrances between chitosans and mucins of the CM. In contrast, entanglements and multiple physical crosslinks between larger chitosan and mucins likely limit their diffusivity. The decrease of chitosan penetration in CM with increasing chitosan molar mass was well corroborated with our previous works on mucin hydrogels *(29)*. Prior to in vivo testing, it was important to validate the use of the jellifying excipient HEC. The addition of such a large hydrated polysaccharide to the formulation, necessary for the vaginal delivery of chitosan, increased the crowding of the formulation which could possibly have affected the ability of chitosan to diffuse into the mucus.

Using in vitro sperm penetration assays, we then found that the CM barrier to sperm could be successfully reinforced by exposure to chitosan solutions. The dependence of the CM barrier reinforcement on chitosan molar mass suggested that there is a minimum chitosan size required to effectively crosslink the mucin strands in the CM. Ovulatory CM is very hydrated with a water content of 97-98% at ovulation *(51)*, and the volume of CM increases 10-20-fold compared to non-ovulatory CM *(52)*. Pore sizes have been estimated to be between 20 and 15,000 nm *(53, 54)*. We hypothesize that oligo-chitosans diffuse and interact with mucins but are unable to bridge over these pores, whereas larger chitosans of 35 kDa, which we expect to be in the order of 100 nm in length *(55)*, could.

We next selected the ewe model to further investigate the efficacy of such an approach. Anatomically, the ewe has been well studied *(56–58)*. The ewe's cervix and vagina share similar epithelial layer thickness compared to humans *(59)*, supporting the use of ewes to test the safety of contraceptive products such as microbicidal vaginal rings *(60)*, and the efficacy of spermicides *(61)*. In addition, the ram deposits semen vaginally *(62)*, not directly in the uterus like in the rat models also used in reproductive and contraceptive research *(63)*. The ewe model also allowed us to track sperm throughout the reproductive tract, which is not easily performed clinically due to invasiveness *(64)*. The chitosan-containing HEC gel reached the cervix after 1 hour but seemed to be halted by the presence of ring structures which are found along the ewe's cervix *(65)*. These ring structures are not found in the human cervix which could mean the formulation could penetrate deeper in humans. Previous studies have shown that viscous gels can penetrate the cervical canal in humans but do not typically reach the uterus in notable amounts *(66–68)*. We showed that the chitosan formulation was effective at reducing the sperm numbers in the distal cervix and uterus of ewes 4 hours after AI and investigated the mechanism by which these effects were obtained. We show that the HEC gel, containing lactic acid and adjusted to pH 5.5 also reduced the average number of sperm detected in the upper reproductive tract, although it was not statistically significantly different from untreated animals. The addition of chitosan was necessary to reach the low sperm counts close to or at 0, suggesting that the mechanism of action was different from pH-deactivation of sperm or the physical blockage of sperm by the HEC gel. This was further confirmed by the absence of effect of chitosan-containing HEC gels on human sperm motility compared to HEC gel alone. Further studies including other viability markers such as membrane integrity, DNA integrity, and ROS production would be required to provide a full toxicology profile of the chitosan towards sperm.

By demonstrating that the barrier can be attributed in large part to the physical reinforcement of the CM barrier, we establish a new mechanism which can be added to the toolbox available for contraceptive design. The contraceptive efficacy of such an approach can only be determined in contraceptives trials, but it is likely that it will in part rely on the natural or induced deactivation of sperm. This is because the chitosan-modified CM will likely be replaced by non-modified CM through the natural mucus turnover, progressively weakening the barrier to sperm. Existing on-demand non-hormonal mechanisms of action seem to show intrinsic limitations which hampers the contraceptive efficacies. Contraceptives such as spermicides, gels and rings, have shown 6-month failure rates of 10-20% *(12, 69)* in typical use, whereas 6-month failure rates are limited to 3-5% for hormonal contraceptives *(70)*. Even when used consistently and correctly, spermicides stay less effective than hormonal treatments *(16)*, with a 6-month failure rate of 4% for spermicides *(71)* versus 0-1% for oral hormonal contraceptives *(72, 73)*. New mechanisms of action, such as the one highlighted in this work, are opportunities to go beyond such a glass ceiling in efficacy.

We also investigated the safety profile of the chitosan-containing gels. Although chitosans are generally biocompatible *(41)*, studies of inflammatory response of cells exposed to chitosan have produced mixed results, likely due to differences in chitosan characteristics. While some studies indicate no effect on fibroblast cells *(74)*, others indicate increase of IL-1α expression from oral epithelial cells *(75)* and mild activation of macrophages cells by pure chitosan *(76)*. In this study, the IL-1α expression induced by chitosan was less than the expression induced by the FDA-approved nonoxynol 9 (N9) spermicide. N9 is known to trigger an inflammatory response, especially in repeated use, characterized by a marked cytotoxicity and the increased secretion of proinflammatory cytokines such as IL-1α and IL1-β from epithelial cell cultures *(40, 77)*. These toxicity markers have been validated in several animal models,

showing epithelial disruption, epithelial cell death, and inflammatory infiltrations when exposed to N-9 *(78–80)*, including using the ewe model *(81)*. In humans, these side effects lead to discomforts *(82)* and are suggested to be linked with increased risk of HIV transmission *(83)*. Thus, these in vitro and in vivo studies suggest that chitosan is unlikely to cause acute toxicity or short-term inflammation of vaginal tissue. The three dimensional cell model used here, although a good mimic of the cell composition and structure of vaginal epithelium *(47)*, does not include the layer of cervical-vaginal secretions, which is likely to bind chitosan and shield the cells from the treatment. Even without mucus secretion, the chitosan, likely due to its negative charge and large size, was restricted to the upper layer of the cells of the in vitro vaginal epithelial tissue.

We have identified several limitations of this study. The ewe model did not not mimic the mechanical shear of intercourse, which can be beneficial by spreading the formulation quickly and helping it reach the cervical mucus, and detrimental by possibly breaking the barrier that was formed. Coitus could therefore be simulated in the ewe model to address this concern *(84)*. Still, even without coitus, because the animals were free to move between interventions, the barrier needed to resist some contractions and resulting mechanical shear generated by the animals. This study does not inform on the contraceptive efficacy of this approach, which will need to be verified, possibly using the ewe model. The safety assessments tests constitute a preliminary assessment of the safety profile of such a treatment. Possible irritation to the vaginal tissues but also cervical and penile tissues will need to be tested in other dedicated in vivo models and in clinical trials. Considering that chitosan formulation could be administered before each intercourse, it is also clear that chronic or sub-chronic toxicity and inflammation will need to be tested. The compatibility with other vaginal gels and devices, and with menstrual bleeding would also need to be addressed during the further development of a chitosan-containing contraceptive vaginal gel. A prolonged presence of the chitosan in the vagina, could also alter the vaginal microbiome. The effect of vaginal products and contraceptives in general has been under-studied but is currently being investigated for hormonal *(85)* and non-hormonal methods *(86)*. Certain chitosans have known antimicrobial activities *(87)* and could affect commensal microbiomes and participate to disbalance, or limit pathogen growth prompting further vaginal microbial health. The antimicrobial activity of chitosan would preferably need to be tested in the in vivo context of the vaginal microbiome, in which secreted mucins and other proteins, lipids, and ions can limit its interaction with microbes.

One other key challenge ahead is the importance of developing the appropriate delivery of the chitosan, which can have a strong impact on efficacy, usability, and overall user compliance. Developers of such a product will need to leverage the conclusions of previous studies on vaginal gels, which have identified ideal volume and rheological properties for optimal coverage of the vaginal wall and cervix *(66, 68, 88)* and modeling work to predict the spreading of vaginal gels *(89)*. The gel can be applied with syringe-type applicators optimized for gel distribution and selected by user preference *(90–92)*.

In conclusion, we demonstrated that certain chitosans can effectively reinforce the cervical mucus barrier to sperm while showing no acute toxicity towards sperm and epithelial cells. Although this study did not demonstrate contraceptive efficacy, we presented a proof of concept for a possible contraceptive mechanism of action, without the potential toxicities of other pericoital methods such as N-9 spermicides. The topical physical reinforcement of the cervical mucus barrier could therefore constitute a class of muco-cervical barrier contraceptives. Similar to hormonal contraceptives which have varied in dose, delivery

modality, and release kinetics since the first approval in the 1960s *(93)*, muco-cervical barrier contraceptives could be derived in various forms, to address the range of user needs in contraception.

Materials and methods

Study design

The details of the study design, analysis and statistics are provided in the sections below. The main goal of this study was to identify chitosan formulation that could successfully block sperm penetration of ovulatory CM. The study first relied on in vitro assays using human ovulatory CM and human sperm, which helped identify chitosan candidates to be further tested in vivo. All experiments were repeated three times with different sperm samples. Although 53 human ovulatory CM samples were collected and analyzed only a fraction could be used for these assays because of limited sample size or quality. For this reason, some of the assay triplicates were performed only on one or two mucus different samples. The in vitro assays also analyzed the diffusion of fluorescently labeled chitosan into the CM.

The sheep model was used to demonstrate the blocking ability of chitosan in vivo. The sheep were Ile de France breed. The sheep model allows the imaging of fluorescently labeled sperm in the vagina, and of sperm up the reproductive tracts on explanted tissues. Animals were allocated to treatment based on age and body condition scores before the day of the experiment to ensure no bias in age or body condition score between the treatment allocations. The body condition scoring technique, scaled from 0 (severe uncondition, or very thin) to 5 (severe overcondition, or obese), allowed us to assess the overall fitness of the ewe, taking into consideration skeletal size, breed, and physiological state. All animals were judged healthy and fit for inclusion prior to using, including lameness. Animals were free of clinical disease, had a condition score of 3 or more, had no obvious signs of damage to the vulva, and had no defects to the udders. All experiments on the ewes were done on the day of ovulation, which is the most challenging time to test such a mucus-reinforcing approach, since the CM is loose and penetrable by sperm. The number of animals for sperm counting was set to at least n=7 based on previous experience of variability of such experiments. The sheep model was also used to assess the acute toxicity of the formulations. In vitro assays complemented the toxicological data, measuring the effect of chitosan formulation on sperm kinematic parameters and viability and cytokine secretion of a commercial three-dimensional vaginal epithelial tissue model.

Chemical and biological agents

Endotoxin-free water (H_2O) was purchased from Merck KGaA. Phosphate-buffered salines (PBS) of pharmaceutical grade and various pH were supplied by Thermo Fisher Scientific or CPAchem Ltd. Lactic acid (LAC) at 32.5 mM and 100 mM was produced by mixing endotoxin-free water (HyClone™ Cell Culture-Grade Water, GE) and 90% lactic acid (Ph.Eur., Fisher Chemical). The adjustment of pH to 5.5 was conducted using 0.1 and 1 M HCl / NaOH (Merck KGaA and CPAchem Ltd.) and 50% NaOH (Sigma-Aldrich).

Chitosan oligomer (CO, 1.4 kDa), chitosan (CS) 95/5 (35.0 kDa), 95/100 (150.0 kDa) and 95/1000 (290.9 kDa) were purchased from Heppe Medical Chitosan GmbH and originated from snow crab chitin. Chitosan derived from the cell wall of fungi Z49 (7.1 kDa), Z56 (18.9 kDa), Z13 (27.9 kDa), and Z10 (36.2 kDa) were purchased from Mycodev Group. All chitosans were more than 90% deacetylated. Hydroxyethyl cellulose (Natrosol® 250 HX Pharm., 10,000 mPa·s, Caesar & Loretz GmbH) was used as a gelling excipient. Fluorogestone acetate vaginal sponge (30 mg) and Pregnant Mare Serum Gonadotropin: Folligon® (PMSG) were purchased from Sanofi Animal Health Ltd. Octadecyl Rhodamine B chloride (O-

246) and MitoTracker Green FM were supplied by Invitrogen. Atto-665 NHS ester was purchased from ATTO-TEC GmbH.

Chitosan labeling, desalting and characterization

Chitosans (CSs) and the chitosan oligomers (CO) were labeled by fluorescein isothiocyanate (FITC, Sigma-Aldrich) for in vitro diffusion testing, using a modified method previously reported in Kootala et al. 2018 *(29)*. Briefly, chitosan was dissolved in 2mL of ultrapure water at 40 mg/ml to which 2 ml of methanol was added. The solution was adjusted the pH to 5.5 with 37% HCl or 2 M NaOH. Then, a solution of 10 mg/ml FITC in DMSO was added to achieve a ratio of 1:50 (1 fluorescein for every 50 repeating units) followed by 2 h of shaking at room temperature in the dark. CSs were precipitated by the successive addition of 2 ml of 2 M NaOH then 4 x 6 ml EtOH, increasing the pH to 9. The supernatant was removed after centrifugation at 20,000 x g for 25 min at 4 °C, and the pellets three times rinsed with ethanol to extract unconjugated FITC. After removing ethanol by rotor vaporization for 2 h, the pellet was frozen with liquid nitrogen, lyophilized and stored at 4 °C.

For in vivo tracking, the chitosan was labeled with Atto-665 dye. Chitosan (m = 3.75 g, c = 35 mg/mL, Heppe Medical Chitosan) was dissolved in an aqueous solution of 100 mM lactic acid overnight. The pH of the solution was adjusted to pH 6 with 0.5 M NaOH. Atto-665 NHS ester (15 mg) was dissolved in 200 µL DMSO and added to the chitosan solution. The solution was stirred for 4 hours at room temperature. Sodium hydroxide (2 mL, 0.5 M) was added to the mixture to raise the pH to a range of 7-8 and precipitate chitosan polymer in large lumps**.** The suspension was transferred into falcon tubes to be centrifuged for 10 min at 4500 rpm. The supernatant was discarded, and precipitates of chitosan were resuspended in Milli-Q water. Suspensions were centrifuged for 10 min at 4500 rpm. Rinsing steps were repeated using ethanol 96% to remove excess of the Atto-dye. Chitosan precipitate was finally rinsed and centrifuged (10 min, 4500 rpm) with Milli-Q water 4 times to remove traces of ethanol. The blue solid was filtered on a Buchner vacuum. Labeled chitosan was freeze-dried to give a colored blue powder as a final product (3.2g, η = 82 %). 1H NMR (400 MHz, D_2O) δ 4.96 – 4.77 (m, 0.6H), 4.3 – 3.32 (m, 4.2H), 3.11 (s, 1H), 1.97 (s, 0.04H).

To desalt the chitosan Z10 (36.2 kDa), a 50mg/ml solution of chitosan was prepared in 32.5 mM lactic acid (LAC). The solution was stirred for 4 h and adjusted in pH to 5.5 by the addition of 1 M HCl. The chitosan solution was purified by dialysis for 5 days (molecular weight cutoff 12-14 kDa, 25 mm, SPECTRA/Por® 4, Spectrum, USA), using ultrapure water adjusted to pH 4.0. The sample was subsequently lyophilized.

The solubility of the chitosan was assessed by transmittance measurements of 5 mg/mL chitosan solutions at 600 nm^2 using a Varian Cary 50 Bio UV-Visible spectrometer and Cary WinUV Simple Reads Software (Agilent Technologies). Samples containing 2.7 % hydroxyethyl cellulose were transferred to a cuvette and centrifuged at 600 x g for 5 min to remove air pockets before turbidity testing. Osmolalities [mOsm/kg H_2O] were determined in 100 µl samples with a Roebling automatic micro-osmometer using freezing point depression. The pH was measured and adjusted with the SevenCompact™ pH S210 meter and pH electrode InLab Ultra-Micro (Mettler Toledo AB). Average molar mass (Mw and Mn) and dispersity (Đ) of chitosans were determined by size-exclusion chromatography (SEC). Deacetylation degree (DDA) of chitosans were determined by proton nuclear magnetic spectroscopy (1H NMR). SEC and 1H NMR spectra were acquired as described elsewhere *(37)*. Results on CO and CS characterization are compiled in Table 2.

Table 2. Characteristics of chitosans and chitosan solutions. The degree in deacetylation (DDA), the weight average (M_w) and number average (M_n) molecular weight, dispersity (Đ, ratio of M_w/M_n), and osmolality in millimole per kilogram water (mOsm/kg H_2O) and measured impurities are shown. The d variability of the values is given as standard deviation. N/A: not analyzed.

Chitosan	DDA	M_w	M_n	Đ	Osmolality at pH 5.5	Impurities
	%	kDa	kDa	-	mOsm/kg H_2O	
0-10 kDa						
CO	78.0	1.4 (±0.7%)	0.9 (±1.3%)	1.6 (±1.5%)	12.3 ± 0.6[a] / 106.3 ± 3.3[b] / 173.7 ± 2.1[d]	2-Propanol, undefined impurities
Z49	98.9	7.1 (±0.4%)	4.8 (±0.7%)	1.5 (±0.9%)	164.7 ± 6.4[d]	Undefined impurities
10-50 kDa						
Z56	93.7	18.9 (±0.3%)	13.1 (±0.4%)	1.4 (±0.5%)	71.7 ± 2.1[c]	Isopropanol, ethanol, methanol
Z13	91.6	27.9 (±0.3%)	21.1 (±0.4%)	1.3 (±0.5%)	70.7 ± 2.1[c]	Isopropanol
95/5	98.5	35.0 (±0.1%)	17.2 (±0.2%)	2.0 (±0.3%)	26.4 ± 2.9[c] / 130.0 ± 1.0[d]	NA
Z10	97.4	36.2 (±0.2%)	27.9 (±0.3%)	1.3 (±0.4%)	105.7 ± 2.9[c]	Isopropanol
$Z10_{desalted}$	95.0	51.2 (±0.4%)	36.9 (±0.5%)	1.4 (±0.7%)	69.3 ± 0.6 [c]	NA
>50 kDa						
95/100	95.0	150.0 (±0.2%)	97.8 (±0.2%)	1.5 (±0.2%)	214.5 ± 12.4[d]	NA
95/1000	94.7	290.9 (±0.4%)	163.4 (±0.4%)	1.8 (±0.6%)	110.7 ± 0.6[d]	NA

[a]Dissolved in endotoxin-free H_2O. [b]Dissolved in 0.05 M phosphate buffered saline. [c]Dissolved in 32.5 mM lactic acid. [d]Dissolved in 100 mM lactic acid. NA = Not Analyzed.

Ram sperm collection and assessment

Ejaculates were obtained from six adult Lacaune rams using an artificial vagina. Semen collection consisted of a pool of one to three successive ejaculates from a given ram, obtained over a 2–5 min period. Semen volume, sperm concentration, and wave motion were assessed immediately after collection. The ejaculate volume was read from a precision balance and the sperm concentration was assessed using a standard pre-calibrated spectrophotometer. Collected semen was deposited on a pre-warmed glass slide and the edge of the drop was observed at low magnification (10X objective) on the thermally controlled stage and wave motion was assessed by phase contrast microscopy *(94)*. Specimens were diluted for stabilization (2-3 h) in a pre-warmed (37 °C) phosphate-buffered saline supplemented with bovine serum albumin (1 mg/ml), obtaining a sperm concentration of 100 mill/ml. To achieve a longer stabilization time of 24 h, raw semen was kept at 15 °C after dilution to 700 million sperm cells/ml in pre-warmed cow milk extender (11.1 g skimmed milk/100 mL of water).

Ewe ovulatory cervical mucus collection and assessment

Cervical mucus was collected at INRAE from ewes before performing sperm penetration assays and was taken from the external orifice of the cervix and the nearby environment by aspiration with a soft catheter connected to a 5 ml syringe.

Chitosan dissolution and formulation

We selected lactic acid solution to solubilize chitosan, because it is naturally present in the human vagina and led to less loosening of the CM network leading to increased sperm migration in the sperm penetration assays than solutions with low osmolalities of 0 and 96 mOsm/kg solutions such as pure water or PBS (**Fig. S9**). All chitosan solutions were at a concentration of 5 mg/mL in 32.5 mM or 100 mM lactic acid (Ph.Eur., Fisher Chemical) and adjusted to pH 5.5 (pH ± 0.02) using 0.1/1 M hydrochloric acid (HCl, Merck KgaA), 0.1/1 M sodium hydroxide (NaOH, CPAchem Ltd.) or 50 % NaOH (Sigma-Aldrich). The pH was selected based on previous reports *(29, 95)* suggesting a high binding capacity for mucin and chitosan.

Chitosan penetration into ovulatory CM

To determine the diffusion distance and amount of chitosan accumulated in ovulatory CM, a modified capillary diffusion assay described by Wu, et al. *(96)* was performed. Cervical mucus was aspirated into two capillaries using customized square capillary tubes (L 60 mm, ID 0.3 x 0.3 mm, OD 0.45 x 0.45 mm, borosilicate glass) with Luer-connector (Hilgenberg GmbH) and 1 ml Soft-Ject syringe (Henke-Sass Wolf GmbH). Next, the tubes were broken off at the Luer-connection, and the broken end was sealed with wax (Paul Marienfeld GmbH & Co. KG). The capillary was gently inserted through the septa of vial caps (55° shore, Teknolab Sorbent AB), puncturing the septum from the inside to the outside with the broken and sealed end of the capillary. The cap with capillary was then screwed onto the glass vial (ND9, 1.5 ml, Avantor) and the open end of the capillary immersed into 300 µl preheated buffer solution or CS-FITC in buffer placed in glass vials. Identical square capillaries without Luer-connector (L 50 mm, ID 0.3 x 0.3 mm, borosilicate glass, CM Scientific Ltd.) filled with CS-FITC solution at 1 or 5 mg/mL were used for calibration. After 30 min incubation at 37 °C and 5% CO_2, the capillaries were observed by fluorescence microscopy and images acquired using a Eclipse Ti inverted microscope with a 2X objective (Nikon), Zyla sCMOS camera (5.5 MP, Andor, Oxford Instruments) and the light source pE-300^{lite} (CoolLED) connected to the NIS-Elements BR 4.60.00 software (Nikon). Images were captured at an exposure time of either 20 ms to avoid saturation, but also at 800 ms to measure low fluorescence signals of the diffusion front deeper inside the capillary (**Fig. S2**). Assays were conducted in triplicate. The limited availability of CM and its limited storage time determined the number of CMs used for the three replicates. Images were analyzed by ImageJ software (version 2.0.0-rc-43/1.52b). A region of interest for fluorescence profiles is a rectangle (h=15, w=1314), in the middle of the capillary starting at 5 mm before the air/CM interface in the capillary. The chitosan concentration estimated based on the calibration capillaries, or the fluorescence intensity normalized to the saturated fluorescence intensity were plotted over the distance in pixels. Each pixel corresponded to 3 µm. At an exposure time of 800 ms, the autofluorescence of buffer-treated CM was subtracted from all measurements.

Sperm penetration assays

Glass vials (ND9, 1.5 ml, VWR) containing micro-inserts (flat bottom, 200 µl, VWR), were filled with 100 µl of lactic acid solution with or without chitosan or with liquefied semen and heated at 37 °C. An aliquot of the transparent section of CM was aspirated into square capillaries ID 0.3 x 0.3 mm and sealed at the broken end. The capillary filled with CM was introduced through the septum of of a cap (55° shore, Teknolab Sorbent AB), with the sealed end first, then the cap was placed on the vial to immerse the capillaries. Non-treated capillaries were directly exposed to semen, and left 30 min at 37 °C. The incubation period was no longer than 30 min to limit the spontaneous loss in sperm motility *(37)*. After incubation, the

capillary penetrated by sperm was removed from the vial through the septum of the cap, stripping sperm and seminal plasma off the capillary's surface. Treated capillaries were first exposed to lactic acid with or without chitosan for 1 min, 5 min, or 30 min at 37 °C, then transferred to a vial containing semen for another 30 minutes at 37°C. To observe the distribution of sperm, a customized microscopic glass slide marked with the distances 0.5, 1, 2, 3, 4 and 5 cm was used. The slides were positioned on a pre-warmed (37 °C) stage heater DC 95 (Linkam Scientific Instruments), and the capillaries positioned onto the glass slide. Videos were recorded at the enumerated distances, including the beginning of the capillary (0.1 cm), using the Eclipse Ci phase contrast microscope (Nikon) equipped with UI-3240LE-C-HQ camera (IDS Imaging Development Systems) using a 10X phase contrast objective (total magnification of 100X), and the software Picsara. The recorded microscopic field was 0.21 x 0.27 mm, equivalent to 0.0567 mm^2. The recording started at the upper, outer surface of the capillary, followed by focusing through the capillary until reaching the lower surface, resulting in a 3-D scan through the capillary (**Movies S3 and S4**). Sperm was counted in the 3-D zone of 0.017 mm^3 corresponding to 17 nl of CM. The assay was conducted in triplicate using the semen of different volunteers.

Sperm penetration assays using ewe ovulatory CM and ram semen were conducted in a similar way than for human samples, albeit using a BH2-RFCA microscope (Olympus) at 10X and Phase 3, and a pco.edge sCMOS camera (Photon Lines) of 10X (total magnification of 100X) and the software CamWare V3.17. Capillary tubes were primarily assessed by phase contrast microscopy, however when assessing chitosan formulated in HEC, the sperm were first stained with DAPI (10 µg/ml, Hoechst Sigma), then observed using the fluorescence mode of the microscope.

In vivo efficacy and safety testing of chitosan formulation in the ewe

Estrus synchronization

A Fluorogestone acetate sponge was inserted in the vagina for 14 days, and 600 IU of PMSG (Pregnant Mare Serum Gonadotropin; Sanofi animal health Ltd.) was intramuscularly injected at the withdrawal of sponges. Oestrus occurred 55 hours after sponge removal.

Sperm collection and labeling

Ejaculates were obtained after natural ejaculation using an artificial vagina. Semen volume and mass motility were assessed immediately after collection. The sperm concentration was assessed using a standard pre-calibrated spectrophotometer. Collected semen was labeled for 8 min with R18 fluorochrome (Invitrogen, O246) and MitoTracker Green FM (Invitrogen, M7514) (300 µM and 20 µM, respectively) according to *(83)*. Semen fluid and dyes were washed out by centrifugation (800 g, 40 min, 37 °C) in a discontinuous Percoll gradient (45% v/v and 90% v/v). Washed spermatozoa were then diluted in a warm (37 °C) skim milk extender (11.1 g/100 mL of water) at a final concentration of 1.0×10^9 sperm/mL. Diluted semen was packaged in 0.25 mL straws and stored at 15 °C until cervical insemination was performed.

Administration of formulation and insemination

The chitosan formulation (5 mL of chitosan-Atto 665 at 5 mg/mL, HEC 2.7% w/w, pH 5.5 in lactic acid) or a formulation without chitosan, (5 mL of HEC 2.7% w/w, pH 5.5 in lactic acid) was deposited in the vagina, using a syringe and a silicone tube extension. The formulation was gently deposited close to the cervix but not into the cervix. The ewes were then set free for one hour, then vaginally inseminated with $1x10^9$ labeled spermatozoa.

pCLE and IVS spectrum assessment of chitosan and sperm penetration in the ewe reproductive tract

In vivo imaging using pCLE.

The distribution of labeled chitosan and labeled sperm was assessed in vivo using probe confocal laser endoscope (pCLE, Cellvizio Dualband, Mauna Kea Technologies). The confocal microprobe delivered laser light at an excitation wavelength of 488 nm and 660 nm and collected emitted fluorescence signal simultaneously from sperm cells in the visible range at 505-633 nm and chitosan in the near infrared range at 673-800 nm. In vivo examination of vagina and cervical os with pCLE, 2 min video sequences were performed before and after vaginal application of formulation and sperm insemination.

Ex vivo imaging using pCLE.

The animals were euthanized by a bolt gun and destruction of the brain via pithing, followed by confirmation of permanent cessation of the circulation 4 hours after sperm insemination. After a 10 min delay following euthanasia, the reproductive tracts of the ewes were collected and dissected. The vagina, posterior cervix, anterior cervix and uterus were dissected for pCLE analysis. A S1500 microprobe (1.5 mm diameter, 3.3 µm lateral resolution) was used for recording 2 min video sequences for each anatomical region (vagina, posterior cervix, anterior cervix and uterus) at a frame rate of 12 images per second. All images from the videos were blindly analyzed by particle tracking analysis software. Sperm cells were quantified using an ImageJ macro (Computer Aided Sperm Analysis, CASA) *(97)* before being manually reviewed to confirm that all particles counted were sperm.

Ex vivo IVIS spectrum imaging on ewe reproductive tracts

Fluorescence imaging on ex vivo ewe reproductive tracts was performed using the Imaging System IVIS® Spectrum (PerkinElmer). Detection and quantification of ATTO 665 from labeled chitosan were obtained after acquisition using the filter pair mode: excitation at 640 nm (bandwidth of 30 nm), and emission at 680 nm (bandwidth of 20 nm). Detection and quantification of octadecyl rhodamine from labeled spermatozoids were performed using the spectral unmixing mode acquisition: excitation at 570 nm (bandwidth of 30 nm), and emission at 620-640-660-680-700 nm (bandwidths of 20 nm). Fluorescent signals and tissue autofluorescence were unmixed. Quantifications of ATTO 665 signal and octadecyl rhodamine signal were applied on vagina, cervix, and uterus regions. Results were expressed in Average Radiant Efficiency [p/s/cm²/sr] / [µW/cm²]. Fluorescent data were uniformly acquired and analyzed with the PerkinElmer Living Image software (version 4.7, Perkin Elmer).

In vitro toxicity profiling

Sperm kinematics

In 50-ml Falcon tubes, fresh human semen (1 ml) was placed on 2ml of a HEC containing 32.5 mM lactic acid (pH 5.5) with or without Z10 chitosan (36.2 kDa) in 50 ml Falcon tubes and incubated at 37 °C. After different time intervals, the semen was sampled (6 µl) and assessed by CASA for sperm count, progressive motility, motility, immotility, velocity, sperm size and cell count as described for semen assessment in Supplementary Materials.

Human vaginal epithelium culture

SkinEthic Human Vaginal Epithelium (HTS 0.33 cm^2) (Episkin), three dimensional models of human vaginal epithelium developed for toxicity testing *(47)*, were cultured in the provided maintenance medium according to the manufacturer's protocol for 24 hours before treatment. The tissue inserts were cultured in a 24-well flat-bottom plate (Corning) in 600 µL of medium and incubated at 37 °C, 5% CO_2. The medium was changed immediately before the treatments.

PrestoBlue™ Cell Viability Assay

Gels composed of chitosan at various concentrations and HEC (2.7% w/v) or N9 (2% v/w) and HEC (2.7% w/v) were prepared, and the pH adjusted to 5.5 with HCl and NaOH. For each gel tested, 250 µL of the gel was applied directly onto the apical side of the tissues and incubated for 24 hours at 37 °C. After the treatments the cell medium on the basal side of the cell culture was removed and 540 µL of fresh SMM medium was added to each well. In each well, 60 µL of the PrestoBlue™ Cell Viability Reagent was added directly to the media (10% v/v) and the plate was incubated for 1 hour at 37 °C. Then, the fluorescence was read on the microplate reader (Biotek, Synergy 4) at an excitation and emission of 560 nm and 590 nm, respectively. Values were corrected for background fluorescence (medium only) and normalized to values of untreated control tissues.

Interleukin release measurements

Twenty-four hours after the treatments of the human vaginal epithelium tissues the cell medium was removed from the 24-well plate. IL-1α release was quantified in the medium by ELISA (DuoSet ELISA, R&D Systems) according to the manufacturer's instructions. The absorbance signal was read at 450 nm using a microplate reader (Biotek, Synergy 4).

Ewe vaginal tissue histology

After a 10 min delay following euthanasia, the reproductive tracts of the ewes were collected and dissected as described above. A biopsy of vaginal tissue of 2x2 cm was cut out (approximately mid-vagina). The tissue biopsy was fixed in 4% paraformaldehyde for up to 72 hours at 4 °C. Following the fixation, the tissues were placed in 1x PBS and stored at 4 °C. The fixed tissues were processed by Histocenter AB. The tissues were dehydrated through a series of ethanol organic solutions (4% formaldehyde 50 °C, 70% ethanol, 2x absolute ethanol, absolute ethanol 65 °C, isopropanol 68 °C, vaporization) and embedded in paraffin in a tissue processor (LOGOS, Milestone MI-61504). Cross sections of the embedded tissues with a 4 µm thickness were cut and mounted on glass slides. The paraffin embedded sections were then stained with Hematoxylin and Eosin in an automated slide stainer (Medite TST 44.200S). The slides were imaged on Pannoramic Scanner P250 (3D Histech) and analyzed using the CaseViewer software (3DHistech). Histopathological analysis was performed by a veterinary toxicopathologist (Atlantic Bone Screen), according to the following scoring system: 1 minimal, 2 slight, 3 moderate, 4 marked, 5 severe.

Statistical analysis

Statistic calculations were conducted with the GraphPad software Prism 9. Normality was examined by the Shapiro-Wilk, D´Agostino & Pearson or Kolmogorov-Smirnov test. The Kruskal-Wallis post-hoc Dunn´s test was performed when data sets did not pass the test for normal distribution. When the values were normally distributed, statistical significance was calculated using either ordinary one-way or two-way analysis of variance (ANOVA). Multiple comparisons were conducted with Tukey´s or Sidak´s test. Significant differences in results are marked as asterisks (P<0.05/0.01/0.001/0.0001 corresponds to

*/**/***/****). The repeatability of results is indicated in figures and tables through calculated standard deviations. The AUC was conveyed as total peak area. To calculate the Top, Bottom, LogIC50 and HillSlope, a curve fitting in the form of the nonlinear regression “sigmoidal, 4PL, X is log(concentration)” was conducted.

List of Supplementary Materials

Materials and methods.
Figure S1 to S10.
Table S1 to S4.
Movie S1 to S4.
Data file S1.

References

1. W. Cates Jr, Family planning: the essential link to achieving all eight Millennium Development Goals. *Contraception* **81**, 460–461 (2010).

2. N. Birdsall, L. A. Chester, Contraception and the status of women: what is the link? *Fam. Plann. Perspect.* **19**, 14–18 (1987).

3. C. Goldin, L. F. Katz, The Power of the Pill: Oral Contraceptives and Women's Career and Marriage Decisions. *J. Polit. Econ.* **110**, 730–770 (2002).

4. J. Bearak, A. Popinchalk, L. Alkema, G. Sedgh, Global, regional, and subregional trends in unintended pregnancy and its outcomes from 1990 to 2014: estimates from a Bayesian hierarchical model. *Lancet Glob Health* **6**, e380–e389 (2018).

5. K. Daniels, W. D. Mosher, Contraceptive methods women have ever used: United States, 1982-2010. *Natl. Health Stat. Report.* , 1–15 (2013).

6. S. G. Chamberlain, K. M. Vogelsong, M. Weinberger, E. Serazin, S. Cairns-Smith, S. E. Gerrard, Reboot contraceptives research — it has been stuck for decades*Nature* **587**, 543–545 (2020).

7. E. G. Raymond, T. Shochet, J. K. Drake, E. Westley, What some women want? On-demand oral contraception. *Contraception* **90**, 105–110 (2014).

8. D. G. Foster, M. A. Biggs, D. Grossman, E. B. Schwarz, Interest in a pericoital pill among women in family planning and abortion clinics. *Contraception* **88**, 141–146 (2013).

9. C. Marshall, S. Guendelman, J. Mauldon, A. Nuru-Jeter, Young Women's Contraceptive Decision Making: Do Preferences for Contraceptive Attributes Align with Method Choice? *Perspect. Sex. Reprod. Health* **48**, 119–127 (2016).

10. G. Larsson, F. Blohm, G. Sundell, B. Andersch, I. Milsom, A longitudinal study of birth control and pregnancy outcome among women in a Swedish population. *Contraception* **56**, 9–16 (1997).

11. J. L. Schwartz, D. H. Weiner, J. J. Lai, R. G. Frezieres, M. D. Creinin, D. F. Archer, L. Bradley, K. T. Barnhart, A. Poindexter, M. Kilbourne-Brook, M. M. Callahan, C. K. Mauck, Contraceptive efficacy, safety, fit, and acceptability of a single-size diaphragm developed with end-user input. *Obstet. Gynecol.* **125**, 895–903 (2015).

12. A. E. Burke, K. Barnhart, J. T. Jensen, M. D. Creinin, T. L. Walsh, L. S. Wan, C. Westhoff, M. Thomas, D. Archer, H. Wu, J. Liu, W. Schlaff, B. R. Carr, D. Blithe, Contraceptive efficacy, acceptability, and safety of C31G and nonoxynol-9 spermicidal gels: a randomized controlled trial. *Obstet. Gynecol.* **116**, 1265–1273 (2010).

13. D. A. Grimes, L. M. Lopez, E. G. Raymond, V. Halpern, K. Nanda, K. F. Schulz, Spermicide used alone for contraception. *Cochrane Database Syst. Rev.* , CD005218 (2013).

14. S. J. Phillips, L. G. Hofler, A. M. Modest, L. F. B. Harvey, L. H. Wu, M. R. Hacker, Continuation of

copper and levonorgestrel intrauterine devices: a retrospective cohort study. *Am. J. Obstet. Gynecol.* **217**, 57.e1–57.e6 (2017).

15. M. Bachofner, K. Blickenstorfer, J. Hutmacher, L. Wehrle, B. Leeners, G. Merki-Feld, Intrauterine device continuation rates and reasons for discontinuation in a Central European clinic with a high standard of care and ultrasound follow-up: a retrospective cohort study. *Eur. J. Contracept. Reprod. Health Care* **23**, 407–414 (2018).

16. D. Mansour, P. Inki, K. Gemzell-Danielsson, Efficacy of contraceptive methods: A review of the literature. *Eur. J. Contracept. Reprod. Health Care* **15**, 4–16 (2010).

17. E. S. Watkins, How the pill became a lifestyle drug: the pharmaceutical industry and birth control in the United States since 1960. *Am. J. Public Health* **102**, 1462–1472 (2012).

18. D. F. Katz, D. A. Slade, S. T. Nakajima, Analysis of pre-ovulatory changes in cervical mucus hydration and sperm penetrability. *Adv. Contracept.* **13**, 143–151 (1997).

19. S. S. Suarez, A. A. Pacey, Sperm transport in the female reproductive tract. *Hum. Reprod. Update* **12**, 23–37 (2006).

20. L. Han, R. Taub, J. T. Jensen, Cervical mucus and contraception: what we know and what we don't. *Contraception* **96**, 310–321 (2017).

21. M. G. Snyder, L. J. Zaneveld, Treatment of cervical mucus with lectins: effect on sperm migration. *Fertil. Steril.* **44**, 633–637 (1985).

22. J. A. Baker, S. L. James, T. Ibrahim, C. Marriott, Alicyclic compounds and their contraceptive use*US Patent* (1991) (available at https://patentimages.storage.googleapis.com/43/14/c3/bcd6a22dd8a633/US4985462.pdf).

23. R. K. Willits, W. M. Saltzman, The effect of synthetic polymers on the migration of monocytes through human cervical mucus. *Biomaterials* **25**, 4563–4571 (2004).

24. A. H. Ansari, K. G. Gould, Contraception and the cervix. *Adv. Contracept.* **2**, 101–115 (1986).

25. T. Crouzier, K. Boettcher, A. R. Geonnotti, N. L. Kavanaugh, J. B. Hirsch, K. Ribbeck, O. Lieleg, Modulating Mucin Hydration and Lubrication by Deglycosylation and Polyethylene Glycol Binding. *Adv. Mater. Interfaces* **2**, 1500308 (2015).

26. T. L. Carlson, J. Y. Lock, R. L. Carrier, Engineering the Mucus Barrier. *Annu. Rev. Biomed. Eng.* **20**, 197–220 (2018).

27. C. Werlang, G. Cárcarmo-Oyarce, K. Ribbeck, Engineering mucus to study and influence the microbiome. *Nature Reviews Materials* (2019) (available at https://www.nature.com/articles/s41578-018-0079-7).

28. I. A. Sogias, A. C. Williams, V. V. Khutoryanskiy, Why is chitosan mucoadhesive? *Biomacromolecules* **9**, 1837–1842 (2008).

29. S. Kootala, L. Filho, V. Srivastava, V. Linderberg, A. Moussa, L. David, S. Trombotto, T. Crouzier, Reinforcing Mucus Barrier Properties with Low Molar Mass Chitosans. *Biomacromolecules* **19**, 872–882 (2018).

30. Y. W. Cho, J. Jang, C. R. Park, S. W. Ko, Preparation and solubility in acid and water of partially deacetylated chitins. *Biomacromolecules* **1**, 609–614 (2000).

31. D. Tien, R. L. Schnaare, F. Kang, G. Cohl, T. J. McCormick, T. R. Moench, G. Doncel, K. Watson, R. W. Buckheit, M. G. Lewis, J. Schwartz, K. Douville, J. W. Romano, In vitro and in vivo characterization of a potential universal placebo designed for use in vaginal microbicide clinical trials. *AIDS Res. Hum. Retroviruses* **21**, 845–853 (2005).

32. V. Insler, H. Melmed, I. Eichenbrenner, D. M. Serr, B. Lunenfeld, The cervical score. *Int. J. Gynaecol. Obstet.* **10**, 223–228 (1972).

33. G. W. Halbert, H. Dobson, J. S. Walton, B. C. Buckrell, The structure of the cervical canal of the ewe. *Theriogenology* **33**, 977–992 (1990).

34. J. D. Swartz, M. Lachman, K. Westveer, T. O'Neill, T. Geary, R. W. Kott, J. G. Berardinelli, P. G. Hatfield, J. M. Thomson, A. Roberts, C. J. Yeoman, Characterization of the vaginal Microbiota of ewes and cows reveals a unique Microbiota with low levels of lactobacilli and near-neutral pH. *Front. Vet. Sci.* **1**, 19 (2014).

35. E. A. Miller, D. E. Beasley, R. R. Dunn, E. A. Archie, Lactobacilli Dominance and Vaginal pH: Why Is the Human Vaginal Microbiome Unique? *Front. Microbiol.* **7**, 1936 (2016).

36. M. J. Wallace-Haagens, B. J. Duffy Jr, H. R. Holtrop, Recovery of spermatozoa from human vaginal washings. *Fertil. Steril.* **26**, 175–179 (1975).

37. U. Schimpf, G. Nachmann, S. Trombotto, P. Houska, H. Yan, L. Björndahl, T. Crouzier, Assessment of Oligo-Chitosan Biocompatibility toward Human Spermatozoa. *ACS Appl. Mater. Interfaces* **11**, 46572–46584 (2019).

38. A. Makler, I. Zaidise, E. Paldi, J. M. Brandes, Factors affecting sperm motility. I. In vitro change in motility with time after ejaculation. *Fertil. Steril.* **31**, 147–154 (1979).

39. S. S. Olmsted, N. H. Dubin, R. A. Cone, T. R. Moench, The rate at which human sperm are immobilized and killed by mild acidity. *Fertil. Steril.* **73**, 687–693 (2000).

40. R. N. Fichorova, L. D. Tucker, D. J. Anderson, The molecular basis of nonoxynol-9-induced vaginal inflammation and its possible relevance to human immunodeficiency virus type 1 transmission. *J. Infect. Dis.* **184**, 418–428 (2001).

41. T. Kean, M. Thanou, Biodegradation, biodistribution and toxicity of chitosan. *Adv. Drug Deliv. Rev.* **62**, 3–11 (2010).

42. T. H. Fischer, R. Connolly, H. S. Thatte, S. S. Schwaitzberg, Comparison of structural and hemostatic

properties of the poly-N-acetyl glucosamine Syvek Patch with products containing chitosan. *Microsc. Res. Tech.* **63**, 168–174 (2004).

43. B. G. Kozen, S. J. Kircher, J. Henao, F. S. Godinez, A. S. Johnson, An alternative hemostatic dressing: comparison of CELOX, HemCon, and QuikClot. *Acad. Emerg. Med.* **15**, 74–81 (2008).

44. J. S. Roberts, J. Niu, J. A. Pastor-Cervantes, Comparison of Hemostasis Times with a Chitosan-Based Hemostatic Pad (Clo-SurPlus Radial™) vs Mechanical Compression (TR Band®) Following Transradial Access: A pilot Study. *Cardiovasc. Revasc. Med.* **20**, 871–874 (2019).

45. B. J. Parker, D. I. Rhodes, C. M. O'Brien, A. E. Rodda, N. R. Cameron, Nerve guidance conduit development for primary treatment of peripheral nerve transection injuries: A commercial perspective. *Acta Biomater.* **135**, 64–86 (2021).

46. Emans, Skaliczki, First-in-human Study to Evaluate a Single Injection of KiOmedineCM-Chitosan for Treating Symptomatic Knee Osteoarthritis. *The Open* (2022) (available at https://openrheumatologyjournal.com/VOLUME/16/ELOCATOR/e187431292206100/FULLTEXT/).

47. S. Ayehunie, C. Cannon, K. Larosa, J. Pudney, D. J. Anderson, M. Klausner, Development of an in vitro alternative assay method for vaginal irritation. *Toxicology* **279**, 130–138 (2011).

48. M. Marczynski, B. T. Käsdorf, B. Altaner, A. Wenzler, U. Gerland, O. Lieleg, Transient binding promotes molecule penetration into mucin hydrogels by enhancing molecular partitioning. *Biomater Sci* **6**, 3373–3387 (2018).

49. M. Marczynski, C. A. Rickert, S. A. Semerdzhiev, W. R. van Dijk, I. M. J. Segers-Nolten, M. M. A. E. Claessens, O. Lieleg, α-Synuclein Penetrates Mucin Hydrogels Despite Its Mucoadhesive Properties. *Biomacromolecules* **20**, 4332–4344 (2019).

50. L. D. Li, T. Crouzier, A. Sarkar, L. Dunphy, J. Han, K. Ribbeck, Spatial Configuration and Composition of Charge Modulates Transport into a Mucin Hydrogel Barrier. *Biophys. J.* **105**, 1357â1365 (2013).

51. L. E. Kopito, H. J. Kosasky, S. H. Sturgis, B. L. Lieberman, H. Shwachman, Water and electrolytes in human cervical mucus. *Fertil. Steril.* **24**, 499–506 (1973).

52. Y. Andersch-Björkman, K. A. Thomsson, J. M. Holmén Larsson, E. Ekerhovd, G. C. Hansson, Large scale identification of proteins, mucins, and their O-glycosylation in the endocervical mucus during the menstrual cycle. *Mol. Cell. Proteomics* **6**, 708–716 (2007).

53. S. S. Olmsted, J. L. Padgett, A. I. Yudin, K. J. Whaley, T. R. Moench, R. A. Cone, Diffusion of macromolecules and virus-like particles in human cervical mucus. *Biophys. J.* **81**, 1930–1937 (2001).

54. P. Vigil, M. E. Cortés, A. Zúñiga, J. Riquelme, F. Ceric, Scanning electron and light microscopy study of the cervical mucus in women with polycystic ovary syndrome. *J. Electron Microsc.* **58**, 21–27 (2009).

55. H. Zhang, Y. Li, X. Zhang, B. Liu, H. Zhao, D. Chen, Directly determining the molecular weight of chitosan with atomic force microscopy. *Front. Nanosci. Nanotechnol* **2**, 123–127 (2016).

56. L. Hympanova, R. Rynkevic, M. G. M. C. Mori Da Cunha, C. M. Diedrich, S. Blacher, L. De Landsheere, K. Mackova, L. Krofta, J.-P. Roovers, J. Deprest, The ewe as an animal model of vaginal atrophy and vaginal Er:YAG laser application. *Menopause* **28**, 198–206 (2020).

57. L. Hympanova, R. Rynkevic, I. Urbankova, S. Blacher, L. de Landsheere, K. Mackova, L. Krofta, J. Deprest, Morphological and Functional Changes in the Vagina following Critical Lifespan Events in the Ewe. *Gynecol. Obstet. Invest.* **84**, 360–368 (2019).

58. L. Abril-Parreño, A. K. Krogenæs, C. J. Byrne, A. Donovan, S. Stuen, E. Caldas, M. Diskin, X. Druart, S. Fair, Ewe breed differences in cervical anatomy and cervicovaginal mucus properties: An international study. *Theriogenology* **160**, 18–25 (2021).

59. K. L. Vincent, N. Bourne, B. A. Bell, G. Vargas, A. Tan, D. Cowan, L. R. Stanberry, S. L. Rosenthal, M. Motamedi, High resolution imaging of epithelial injury in the sheep cervicovaginal tract: a promising model for testing safety of candidate microbicides. *Sex. Transm. Dis.* **36**, 312–318 (2009).

60. J. D. S. Holt, D. Cameron, N. Dias, J. Holding, A. Muntendam, F. Oostebring, P. Dreier, L. Rohan, J. Nuttall, The sheep as a model of preclinical safety and pharmacokinetic evaluations of candidate microbicides. *Antimicrob. Agents Chemother.* **59**, 3761–3770 (2015).

61. Y. Zhu, J. Saada, S. Bhawana, S. Lai, P. Villarreal, R. Pyles, M. Motamedi, G. Vargas, T. Moench, K. L. Vincent, Surrogate post-coital testing for contraceptive efficacy against human sperm activity in the ovine vaginal model†. *Biol. Reprod.* **104**, 317–324 (2021).

62. H. W. Hawk, Sperm survival and transport in the female reproductive tract. *J. Dairy Sci.* **66**, 2645–2660 (1983).

63. J. W. Overstreet, G. W. Cooper, Sperm transport in the reproductive tract of the female rabbit: I. The rapid transit phase of transport. *Biol. Reprod.* **19**, 101–114 (1978).

64. C. M. Glazener, W. C. Ford, M. G. Hull, The prognostic power of the post-coital test for natural conception depends on duration of infertility. *Hum. Reprod.* **15**, 1953–1957 (2000).

65. J. Moré, Anatomy and histology of the cervix uteri of the ewe: new insights. *Acta Anat.* **120**, 156–159 (1984).

66. K. T. Barnhart, E. S. Pretorius, K. Timbers, D. Shera, M. Shabbout, D. Malamud, In vivo distribution of a vaginal gel: MRI evaluation of the effects of gel volume, time and simulated intercourse. *Contraception* **70**, 498–505 (2004).

67. K. T. Barnhart, E. S. Pretorius, K. Timbers, D. Shera, M. Shabbout, D. Malamud, Distribution of a 3.5-mL (1.0%) C31G vaginal gel using magnetic resonance imaging. *Contraception* **71**, 357–361 (2005/5).

68. E. S. Pretorius, K. Timbers, D. Malamud, K. Barnhart, Magnetic resonance imaging to determine the distribution of a vaginal gel: before, during, and after both simulated and real intercourse. *Contraception* **66**, 443–451 (2002).

69. K. T. Barnhart, M. J. Rosenberg, H. T. MacKay, D. L. Blithe, J. Higgins, T. Walsh, L. Wan, M. Thomas, M. D. Creinin, C. Westhoff, W. Schlaff, D. F. Archer, C. Ayers, A. Kaunitz, S. Das, T. R. Moench, Contraceptive efficacy of a novel spermicidal microbicide used with a diaphragm: a randomized controlled trial. *Obstet. Gynecol.* **110**, 577–586 (2007).

70. K. Kost, S. Singh, B. Vaughan, J. Trussell, A. Bankole, Estimates of contraceptive failure from the 2002 National Survey of Family Growth*Contraception* **77**, 10–21 (2008).

71. K. Barnhart, C. Dart, K. Culwell, Efficacy, Safety, and Acceptability of Acidform (Amphora) and Nonoxynol-9 Contraceptive Vaginal Gels [16N]. *Obstetrics & Gynecology* **127**, 118S (2016).

72. S. T. Nakajima, D. F. Archer, H. Ellman, Efficacy and safety of a new 24-day oral contraceptive regimen of norethindrone acetate 1 mg/ethinyl estradiol 20 µg (Loestrin® 24 Fe)*Contraception* **75**, 16–22 (2007).

73. H. Ferguson, M. L. Vree, J. Wilpshaar, T. K. Eskes, Multicenter study of the efficacy, cycle control and tolerability of a phasic desogestrel-containing oral contraceptive. *Eur. J. Contracept. Reprod. Health Care* **5**, 35–45 (2000).

74. T. Mori, M. Okumura, M. Matsuura, K. Ueno, S. Tokura, Y. Okamoto, S. Minami, T. Fujinaga, Effects of chitin and its derivatives on the proliferation and cytokine production of fibroblasts in vitro. *Biomaterials* **18**, 947–951 (1997).

75. H. S. Anggani, E. Hasriati, E. Winiati Bachtiar, Evaluation of IL-1α and IL-1β, COX-2, and iNOS mRNA Expression in Orthodontic Patients Given Chitosan Mouthwash During Treatment with Miniscrew. *J Int Soc Prev Community Dent* **11**, 561–565 (2021).

76. C. L. Bueter, C. K. Lee, J. P. Wang, G. R. Ostroff, C. A. Specht, S. M. Levitz, Spectrum and mechanisms of inflammasome activation by chitosan. *J. Immunol.* **192**, 5943–5951 (2014).

77. D. L. Patton, S. K. Wang, C. C. Kuo, In vitro activity of nonoxynol 9 on HeLa 229 cells and primary monkey cervical epithelial cells infected with Chlamydia trachomatis. *Antimicrob. Agents Chemother.* **36**, 1478–1482 (1992).

78. B. J. Catalone, T. M. Kish-Catalone, L. R. Budgeon, E. B. Neely, M. Ferguson, F. C. Krebs, M. K. Howett, M. Labib, R. Rando, B. Wigdahl, Mouse model of cervicovaginal toxicity and inflammation for preclinical evaluation of topical vaginal microbicides. *Antimicrob. Agents Chemother.* **48**, 1837–1847 (2004).

79. D. L. Patton, G. G. Kidder, Y. C. Sweeney, L. K. Rabe, S. L. Hillier, Effects of multiple applications of benzalkonium chloride and nonoxynol 9 on the vaginal epithelium in the pigtailed macaque (Macaca nemestrina). *Am. J. Obstet. Gynecol.* **180**, 1080–1087 (1999).

80. P. Eckstein, M. C. Jackson, N. Millman, A. J. Sobrero, Comparison of vaginal tolerance tests of spermicidal preparations in rabbits and monkeys. *J. Reprod. Fertil.* **20**, 85–93 (1969).

81. K. L. Vincent, G. Vargas, J. Wei, N. Bourne, M. Motamedi, Monitoring vaginal epithelial thickness changes noninvasively in sheep using optical coherence tomography. *Am. J. Obstet. Gynecol.* **208**, 282.e1–7 (2013).

82. M. K. Stafford, H. Ward, A. Flanagan, I. J. Rosenstein, D. Taylor-Robinson, J. R. Smith, J. Weber, V. S. Kitchen, Safety study of nonoxynol-9 as a vaginal microbicide: evidence of adverse effects. *J. Acquir. Immune Defic. Syndr. Hum. Retrovirol.* **17**, 327–331 (1998).

83. L. Van Damme, G. Ramjee, M. Alary, B. Vuylsteke, V. Chandeying, H. Rees, P. Sirivongrangson, L. M. Tshibaka, V. Ettiègne-Traoré, C. Uaheowitchai, S. S. A. Karim, B. Mâsse, J. Perriëns, M. Laga, Effectiveness of COL-1492, a nonoxynol-9 vaginal gel, on HIV-1 transmission in female sex workers: a randomised controlled trial. *Lancet* **360**, 971–977 (2002).

84. B. Shrestha, A. Schaefer, Y. Zhu, J. Saada, T. M. Jacobs, E. C. Chavez, S. S. Omsted, C. A. Cruz-Teran, G. B. Vaca, K. Vincent, T. R. Moench, S. K. Lai, Engineering sperm-binding IgG antibodies for the development of an effective nonhormonal female contraception. *Sci. Transl. Med.* **13** (2021)

85. J. P. Brooks, D. J. Edwards, D. L. Blithe, J. M. Fettweis, M. G. Serrano, N. U. Sheth, J. F. Strauss 3rd, G. A. Buck, K. K. Jefferson, Effects of combined oral contraceptives, depot medroxyprogesterone acetate and the levonorgestrel-releasing intrauterine system on the vaginal microbiome. *Contraception* **95**, 405–413 (2017).

86. N. Kancheva Landolt, S. Chaithongwongwatthana, S. Nilgate, N. Teeratakulpisarn, S. Ubolyam, T. Apornpong, J. Ananworanich, N. Phanuphak, HIVNAT 199 study team, Use of copper intrauterine device is not associated with higher bacterial vaginosis prevalence in Thai HIV-positive women. *AIDS Care* **30**, 1351–1355 (2018).

87. E. I. Rabea, M. E.-T. Badawy, C. V. Stevens, G. Smagghe, W. Steurbaut, Chitosan as antimicrobial agent: applications and mode of action. *Biomacromolecules* **4**, 1457–1465 (2003).

88. C. K. Mauck, D. Katz, E. P. Sandefer, M. D. Nasution, M. Henderson, G. A. Digenis, I. Su, R. Page, K. Barnhart, Vaginal distribution of Replens and K-Y Jelly using three imaging techniques. *Contraception* **77**, 195–204 (2008).

89. D. F. Katz, A. Yuan, Y. Gao, Vaginal drug distribution modeling. *Adv. Drug Deliv. Rev.* **92**, 2–13 (2015).

90. M. E. LePage, D. Brown Jr, J. Wells, Patient acceptance of prefilled disposable vaginal applicator. *Am. J. Obstet. Gynecol.* **158**, 1006–1008 (1988).

91. R. F. Omar, S. Trottier, G. Brousseau, C. Ouellet, A. Danylo, T. Ong, M. G. Bergeron, Universal vaginal applicator for the uniform distribution of vaginal gel and cream formulations: a magnetic resonance imaging study. *J. Obstet. Gynaecol. Can.* **36**, 42–50 (2014).

92. A. J. Bakke, T. Zaveri, M. J. Higgins, G. R. Ziegler, J. E. Hayes, Design aspects of vaginal applicators that influence acceptance among target users. *Sci. Rep.* **11**, 9802 (2021).

93. R. Sitruk-Ware, A. Nath, D. R. Mishell Jr, Contraception technology: past, present and future. *Contraception* **87**, 319–330 (2013).

94. I. David, P. Kohnke, G. Lagriffoul, O. Praud, F. Plouarboué, P. Degond, X. Druart, Mass sperm motility is associated with fertility in sheep. *Anim. Reprod. Sci.* **161**, 75–81 (2015).

95. K. Haugstad, A. Håti, C. Nordgård, P. Adl, G. Maurstad, M. Sletmoen, K. Draget, R. Dias, B. Stokke, Direct Determination of Chitosan–Mucin Interactions Using a Single-Molecule Strategy: Comparison to Alginate–Mucin Interactions. *Polymers* **7**, 161–185 (2015).

96. N. Wu, X. Zhang, F. Li, T. Zhang, Y. Gan, J. Li, Spray-dried powders enhance vaginal siRNA delivery by potentially modulating the mucus molecular sieve structure. *Int. J. Nanomedicine* **10**, 5383–5396 (2015).

97. J. G. Wilson-Leedy, R. L. Ingermann, Development of a novel CASA system based on open source software for characterization of zebrafish sperm motility parameters. *Theriogenology* **67**, 661–672 (2007).

98. W. Health Organization, WHO laboratory manual for the examination and processing of human semen, (2010) (available at https://apps.who.int/iris/bitstream/handle/10665/44261/9789750011245_tur.pdf).

99. L. Björndahl, What is normal semen quality? On the use and abuse of reference limits for the interpretation of semen analysis results, *Hum. Fertil.* **14**, 179–186 (2011).

100. B. T. Henry, J. Adler, S. Hibberd, M. S. Cheema, S. S. Davis, T. G. Rogers, Epi-fluorescence microscopy and image analysis used to measure diffusion coefficients in gel systems, *J. Pharm. Pharmacol.* **44**, 543–549 (1992).

Acknowledgements
We thank K. Magnusson for assurance with the manual semen analysis. M. Fursätter is acknowledged for her assistance with the management and screening of female volunteers and the CM collection. We are grateful to G. Nachmann, T. Arvidson and S. Konstholm for assistance with the analysis of chitosan penetration into mucus. We also acknowledge L. Jakobsson for her assistance with the chitosan diffusion assays through image acquisition and analysis. And thank you to K.G. Danielsson for their valuable comments on the manuscript.

Author contributions
Ulrike Schimpf has established a sperm penetration assay, and designed experiments, collected and analyzed data on chitosan diffusion and sperm penetration into mucus. She has plotted all data from the

manuscript, designed and generated the figures, and wrote the manuscript. Gilai Nachmann has assisted with the characterization of cervical mucus, and the assessment of chitosan diffusion through cervical mucus. Erika Caldas-Silveira, Isabelle Lantier, Xavier Druart, Ljudmila Katchan, and Thomas Crouzier have designed the in vivo experiments in the sheep. Erika Caldas-Silveira has performed and analyzed all in vivo experimentation in the sheep. Isabelle Lantier, has collected and analyzed the chitosan spreading data in the sheep. Ulrike Schimpf, Stéphane Trombotto, and Cécile Vigier-Carriere have contributed to the characterization of the chitosans used in this study. Sebastian Gidlöf and Aino Fianu Jonasson have assisted with human ovulatory cervical mucus collection and assessment. Lars Björndahl has assisted with the design of experiments involving human sperm collection, characterization and the sperm penetration assay. The toxicology work was performed by U.S for all in vitro sperm viability assessments, and by L.K for the mammalian cell cytotoxicity assessment. Thomas Crouzier has provided funding, supervision, and wrote the manuscript.

Competing interests

TC, UC, CVC, LK hold shares of the Cirqle Biomedical Contraception ApS company and are associated with the company through employment or consulting contracts. Cirqle Biomedical Contraception ApS is developing a contraceptive based on the mechanism of action described in this manuscript. A patent was filed: A vaginal contraceptive composition for reinforcement of mucus barrier properties, Thomas Crouzier and Ulrike Schimpf, PCT WO2021069046A1.

Data and materials availability

All data associated with this study are present in the paper or supplementary materials.
MATLAB 2018 Code: DOI 10.5281/zenodo.7297781 (Zenodo)

Supplementary Materials

Topical reinforcement of the cervical mucus barrier to sperm

Ulrike Schimpf[1, 2Ψ]*, Erika Caldas-Silveira[3Ψ], Ljudmila Katchan[4], Cécile Vigier-Carriere[4], Isabelle Lantier[5], Gilai Nachmann[1], Sebastian Gidlöf[6,7], Aino Fianu Jonasson[6,7], Lars Björndahl[8], Stéphane Trombotto[9], Xavier Druart[3], Thomas Crouzier[1,4,10,11]*

[1]Division of Glycoscience, Department of Chemistry, School of Engineering Science in Chemistry, Biotechnology and Health (CBH), AlbaNova University Center, KTH Royal Institute of Technology, 106 91 Stockholm, Sweden
[2]Department of Material and Environmental Chemistry (MMK), Stockholm University, 106 91 Stockholm, Sweden
[3]PIXANIM, Physiologie de la Reproduction et des Comportements, UMR INRAE, CNRS, Université de Tours, IFCE, 37380 Nouzilly, France
[4]Cirqle Biomedical Contraception ApS, Ole Maaløes Vej 3, 2200 Copenhagen, Denmark
[5]French National Institute for Agriculture, Food, and Environment (INRAE), UMR ISP, Université de Tours, 37380 Nouzilly, France
[6]Department of Gynecology and Reproductive Medicine, Karolinska University Hospital, 141 86 Stockholm, Sweden
[7]Department of Clinical Science, Intervention and Technology (CLINTEC), Karolinska Institutet, Alfred Nobels alle 8, 141 52 Huddinge, Sweden
[8]ANOVA - Andrology, Sexual Medicine, Transmedicine, Karolinska University Hospital and Karolinska Institutet, Norra Stationsgatan 69, 113 64 Stockholm, Sweden
[9]Ingénierie des Matériaux Polymères (IMP), CNRS UMR 5223, Université Claude Bernard Lyon 1, 69622 Villeurbanne, France
[10]AIMES - Center for the Advancement of Integrated Medical and Engineering Sciences at Karolinska Institutet and KTH Royal Institute of Technology, 171 77 Stockholm, Sweden
[11]Department of Neuroscience, Karolinska Institutet, 171 77 Stockholm, Sweden

[Ψ]Co-first authorship
*Corresponding authors:
Thomas Crouzier: crouzier@kth.se
Ulrike Schimpf: schimpf@kth.se

Materials and methods

Collection and assessment of human sperm

Semen of patients and volunteers in the age of 18-45 years were collected at the ANOVA andrology clinic (Solna, Sweden), and were applied in basic semen analyses and penetration assays not later than 3 h after collection. Each patient and volunteer signed an informed consent. Studies were approved by the relevant ethical committee (EPN, No.: 2015/2326-31 and 2019-02466), Stockholm (Sweden). Data were obtained for the collection time, abstinence time and semen volume. Semen was gently liquefied for 30 min on a rocker in an incubation chamber heated up to 37 °C, after complete collection of ejaculates by masturbation. Microscopic analysis was conducted by pipetting 6 µl semen in pre-warmed Leja (Netherland) counting chamber slides (20 micron). Next, specimens were assessed via clinical ECLIPSE 50i microscope (Nikon Instruments) equipped with stage heater MS 100 (37 °C, Linkam Scientific Instruments), 10X objective (Ph1) and 0.5X charge coupled device camera UI-1540LE-M-HQ (IDS Imaging Development Systems GmbH) with total magnification of 5X. The system was connected to the Computer Aided Semen Analysis software QualiSperm (v3.0.9.486, AKYmed). In addition to the sperm concentration [10^6/ml], the progressive motility [%] (Class A, sperm that move forward with a speed of >25 µm/s), motility [%] (Class A (>25 µm/s) + Class B (5-25 µm/s) + Class C (0-5 µm/s)), immotility [%], average path velocity [µm/s], sperm size [μm^2] and number of cells were measured (**Table S1**). Semen samples meeting the following criteria were included in this study: volume of >1.5 ml, concentration of >15x10^6/ml and >40% progressive motility. These criteria reflect reference limits of the World Health Organization (WHO) *(98)* and as stated elsewhere *(99)*. In each run ten values were generated by assessing 5 fields in two chambers. Mean values and corresponding standard deviations are presented.

Collection and assessment of human cervical mucus

Ovulatory cervical mucus (CM) was collected at the Karolinska University Hospital Huddinge (Sweden) and applied in scientific studies after receiving ethical approval by the Stockholm County ethical committee (EPN, No.: 2017/703-31 and 2018/850-32), Stockholm (Sweden), and agreements signed by female volunteers. Women undergoing the procedure were not using hormonal contraceptives, between 18 and 30 years old, had a BMI of 19-25, were non-smokers, had regular menstruation (25-35 d), and were neither under medication nor affected by chronic diseases. Ovulation was indicated by at-home Clearblue digital ovulation tests, then measurement of blood FSH, LH and estradiol concentrations which indicate the occurrence of ovulation.

At the collection, the gaping of the external orifice was assessed, and the endometrial thickness measured by ultrasound scan. Mucus was collected at the external orifice using the endometrial catheters Gynebiops standard CH9 (GYNEAS) and Pipelle de Cornier for endometrial biopsy (PRODiMED) with known radius (r). The amount of CM was obtained by reading of the catheters length (L) filled with mucus and calculating the volume (V) by $V = \pi \times r^2 \times L$. Specimens were stored at 4 °C until further tests and no longer than 30 days. Neither the sperm penetrability of untreated CM, nor the barrier reinforcement effect by chitosans larger than 7 kDa was affected by mucus age (**Figure S10**). This was independent of the quality of the semen used in each experiment.

For further valuation, aliquots of the CM were transferred onto a microscopic slide (76x26 mm, Gerhard Menzel B.V. & Co. KG) to investigate the spinnability by stretching mucus drops between microscopic

slide and cover glass (22x22 mm, Gerhard Menzel B.V. & Co. KG) under notation of mucus thread length. Wet preparations for microscopy were prepared to examine the cellularity via inverted laboratory microscope DM IL LED (5W, Leica Microsystems GmbH), 10X objective and 10X camera DFC295 (3 Megapixel) with total magnification of 100X, connected to the software Leica Application Suite (LAS) 4.1.0. Contaminations by bacteria, fungi, parasites or dead sperm cells were determined. Next, objective slides were removed, forming a mucus smear for air drying of specimens to assess the extent of ferning and type of mucus phases per 40X objective (total magnification of 400X). The remaining CM was transferred into Eppendorf tubes and the pH measured as described above. After an assessment of the gaping, quantity, spinnability and ferning a cervix score was calculated. Each category was valued with 1 (poor), 2 (moderate) or 3 (good) points. An Insler score of ≦7, 8-10 or 11-12 represented insufficient, good or excellent specimens. These data (**Table S2**) provided a preliminary assessment of the penetrability of cervical mucus for sperm.

Analysis of the chitosan gradient in human ovulatory CM

A MATLAB 2018 (MathWorks) script was used to analyze fluorescence intensity profiles of capillaries into which chitosan diffused to distinguish between saturation, gradient and absence of fluorescence signals in capillaries filled with CS-FITC and an exposure time of 800 ms. These calculations required the input of the sigmoidal (4 parameter logistic distribution) non-linear regression of each fluorescence intensity profiles, which was first calculated in the Prism software. The values of the maximum, minimum, LogIC50 and HillSlope were manually inserted in the MATLAB 2018 code (available doi: 10.5281/zenodo.7297781) to calculate the first and second drop of fluorescence intensity:

$$RFI = Bottom + \frac{Top - Bottom}{1 + 10^{Hill\ slope\ x\ (LogIC50 - Distance)}}$$

$$\frac{d^2RFI}{dDistance^2} = \frac{ln^2(10) \times (Hill\ slope)^2 \times (Top - Bottom) \times (10^{2 \times Hill\ Slope \times (LogIC50 - Distance)} - 10^{Hill\ Slope \times (LogIC50 - Distance)})}{(10^{Hill\ Slope \times (LogIC50 - Distance)} + 1)^3}$$

The first and second drop describe the values at which the saturation ends and the absence of chitosan begins. CS-FITC concentrations were expressed as a function of distance [mm]. By that, the maximum saturation and gradient were obtained.

In addition, the diffusion coefficient (D) was calculated in accordance to Henry et al. *(100)*. The resulting pixel numbers and RFUs of curves acquired at 20 ms were normalized to 100, and the normalized RFUs obtained at 50 pixels applied in the following calculation for D [mm^2/s]:

$$D = \frac{\left(\frac{(Normalized\ RFU\ x\ 3)}{(2\ x\ 0.476936)}\right)^2}{1800\ x\ 10^6}$$

Figures

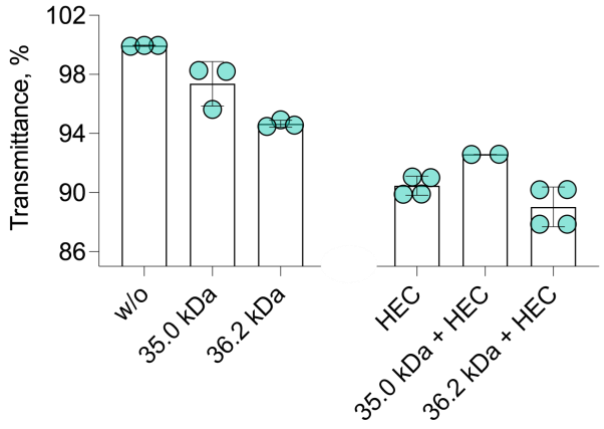

Figure S1. Solubility of chitosan with and without the addition of hydroxyethyl cellulose. The solubility of the 35.0 and 36.2 kDa chitosans with or without hydroxyethylcellulose (HEC) in 32.5 mM lactic acid as assessed by transmittance measurements, with a 32.5 mM lactic acid solution as a reference (w/o). Mean values and standard deviation from the mean from at least two independent samples are shown. The absence of statistical difference between w/o or HEC and chitosan solutions with or without HEC were tested via the Shapiro-Wilk test followed by the Dunn's test.

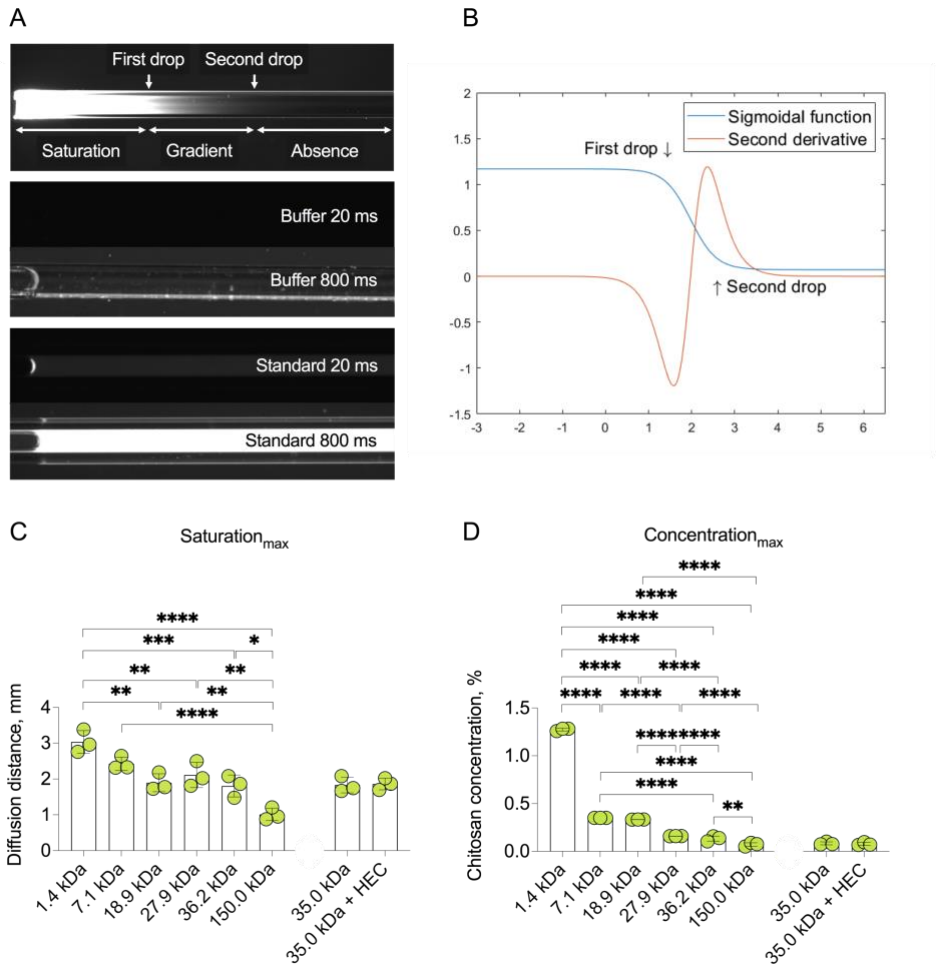

Figure S2. Diffusion assay references, functions and maximum saturation and chitosan concentration in capillary tubes. A) Visual description of the first and second drop in fluorescence intensity for CM-filled capillaries including the buffer and standard solution controls. **B**) In blue, the sigmoidal function (4 parameter logistic distribution) from the non-linear regression of 800 milliseconds. (ms) exposure rate, and in orange, the second derivative of the function. **C**) Diffusion distance of chitosan based on 800 ms exposure. **D**) Concentration of chitosan absorbed based on area under the curve of 20 ms exposure. Each measurement made with CM was conducted with the CM collected from one or more donors. The graphs represent individual values, their mean values and the standard deviation. Statistical differences between groups were tested using the Shapiro-Wilk test followed by Tukey's test. Asterisks denote significant increases or decreases (*P<0.05, **P<0.01, ***P<0.001, ****P<0.0001).

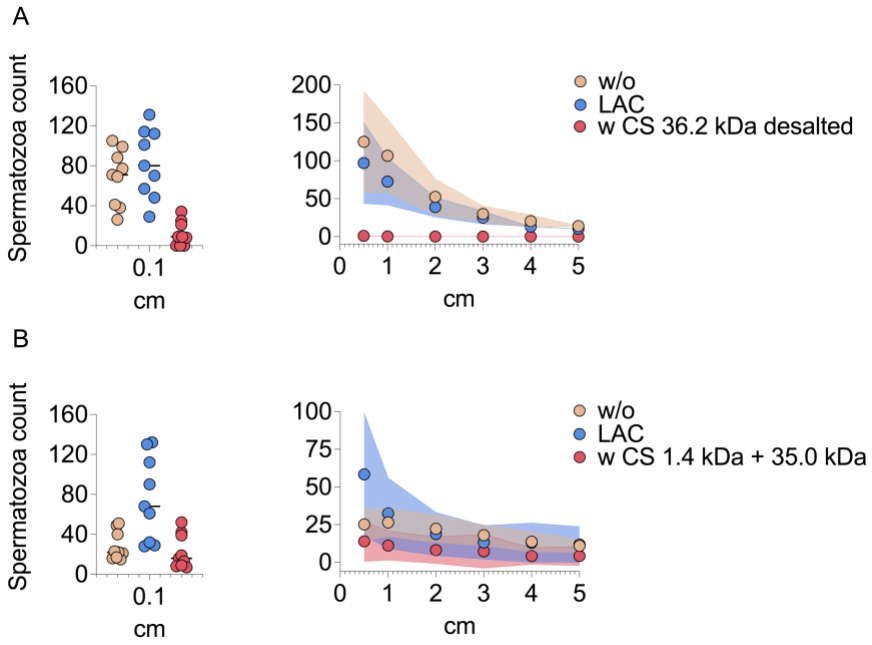

Figure S3. Effect of desalting chitosan solution and combining low- and medium-weight chitosans on sperm penetration. Sperm penetration assay was performed on human ovulatory CM. The mucus was either untreated (w/o), treated with a 32.5 mM pH 5.5 lactic acid solution (LAC) or with a chitosan solution in lactic acid (5 mg/mL total chitosan concentration in 32.5 mM lactic acid, pH 5.5). The measurements were conducted with **A**) 36.2 kDa chitosan previously dialyzed to remove associated salts (see materials and methods, section 3.2), **B**) or a mixture of low (1.4 kDa) and medium weight chitosan (35 kDa). Each measurement was performed in triplicate, using one or more CM samples and at least two sperm donors. Replicates are the mean of the sperm count at three different fields at each distance. In the left graphs the median is shown. In the right graphs each point is the mean of three measurements, and the colored area represents the standard deviation of the mean.

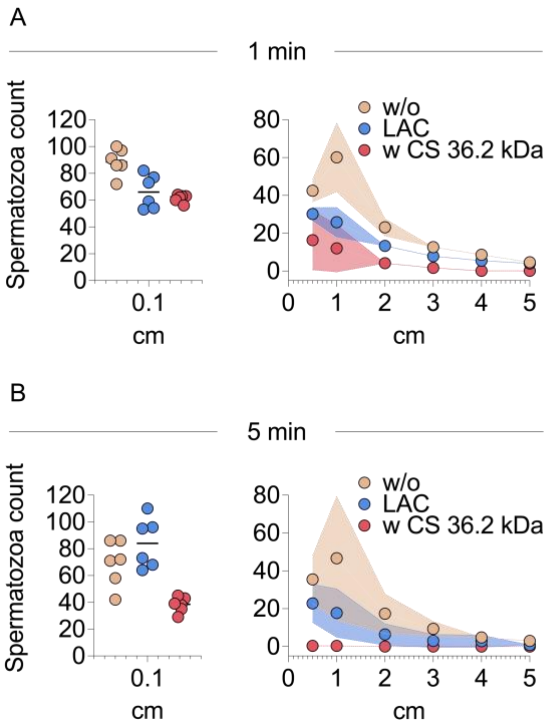

Figure S4. Short-term treatments with chitosan to reveal the time onset of effective barrier reinforcement. Sperm penetration assays were performed as described in the Materials and Methods section but with the contact time between the chitosan solution and the CM adjusted to either **A**) 1 minute or **B**) 5 minutes instead of 30 minutes. Each measurement was conducted in duplicate, using two individual CM and two semen from one sperm donor. Replicates are the mean of the sperm count at three different fields at each distance. In the left graphs the median is shown. In the right graph each point is the mean of three measurements, and the colored area represents the standard deviation of the mean.

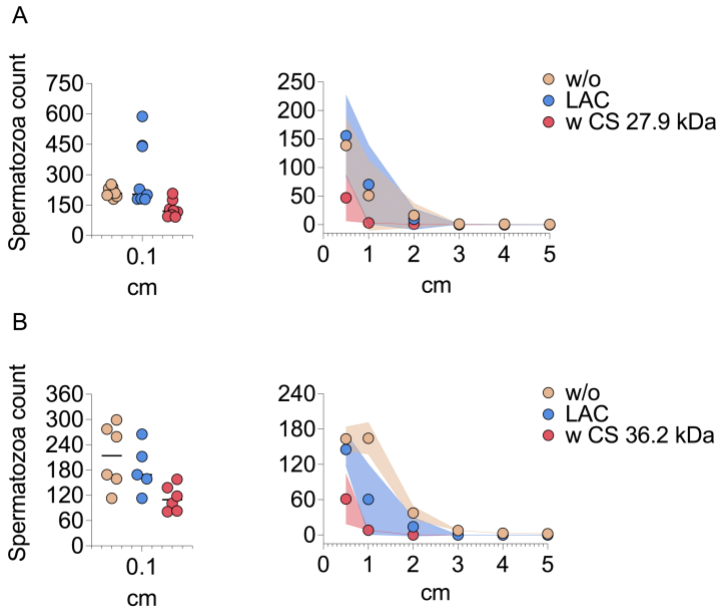

Figure S5. In vitro validation of chitosan barrier-reinforcing properties on ewe cervical-vaginal mucus. The sperm penetration assay was performed using ovulatory cervical-vaginal secretions collected from ovulating ewes. The mucus was either untreated (w/o), treated with a 32.5 mM pH 5.5 lactic acid solution (LAC) or with a chitosan solution in lactic acid (5 mg/mL chitosan in 32.5 mM lactic acid, pH 5.5). The measurements were conducted with **A**) the 27.9 kDa chitosan and **B**) the 36.2 kDa chitosan. Each measurement was performed in duplicate (CS 36.2 kDa) or triplicate (CS 27.9 kDa), using one or more cervical mucus samples. Replicates are the mean of the sperm count at three different fields at each distance. In the left graphs the median is shown. In the right graphs each point is the mean of three measurements, and the colored area represents the standard deviation of the mean.

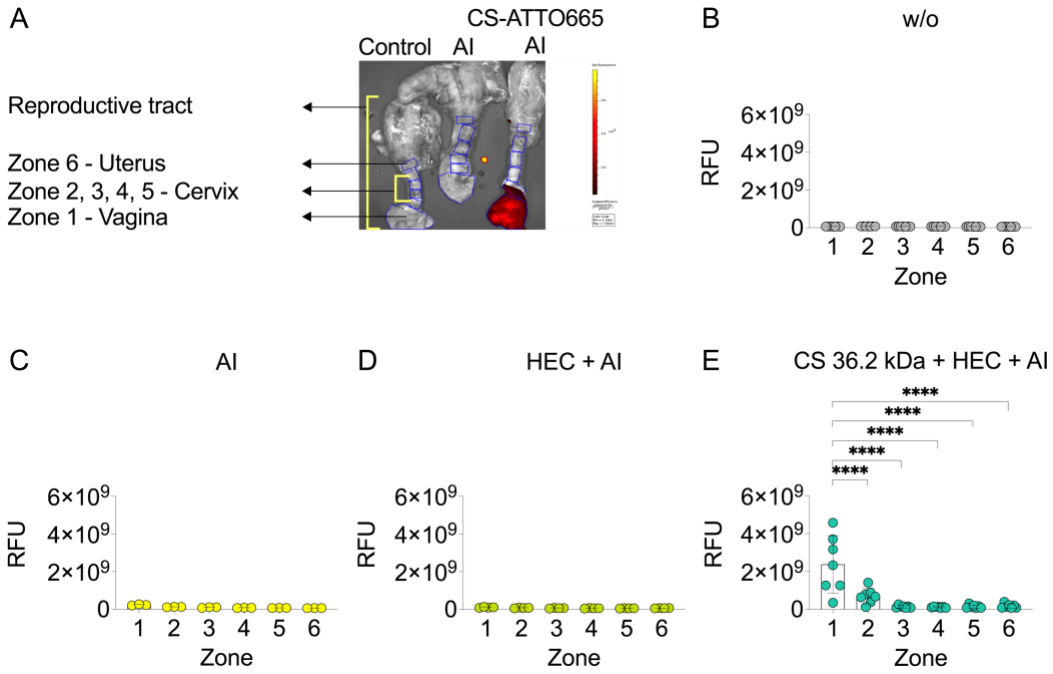

Figure S6. Distribution of the chitosan gel formulation through the reproductive tract of the ewe 4 hours after administration of vaginal formulations. A) The chitosan was labeled with Atto-665 dye (red color) to enable its tracking. Then the fluorescence of the tissue is measured using an In Vivo Imaging System (IVIS Spectrum, PerkinElmer). **B**) The relative fluorescence units (RFU) of the tract without treatment (w/o, *n*=7 ewes), **C**) without treatment but following artificial insemination using unlabeled sperm (AI, *n*=3 ewes), **D**) treated with a hydroxyethyl cellulose gel (HEC, *n*=4 ewes) and AI, and **E**) after treatment with a HEC gel containing the labeled chitosan and followed by AI (CS 36.2 kDa + HEC + AI, *n*=7 ewes). The measurements conducted in B to D serve as controls and demonstrate that semen and HEC exhibit no autofluorescence that interferes with the fluorescence emitted by the labeled chitosan. The graphs represent individual values, their mean values and the standard deviation. Statistical differences were tested using the Shapiro-Wilk test followed by the Tukey's test. Asterisks denote significant increases or decreases (****P<0.0001).

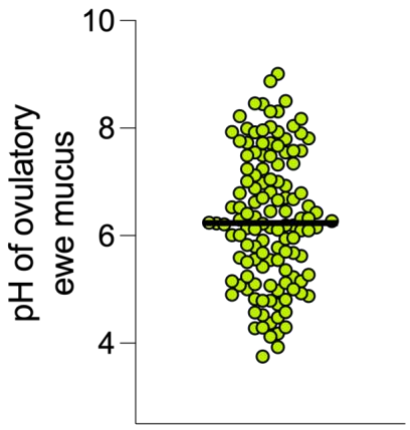

Figure S7. pH of the ovulatory ewe cervical mucus collected before administration of the formulation. The data represented is a collection of measurements performed on 126 different ovulating ewes, performed a maximum of 8 hours after collection of the cervical-vaginal secretion from the ewes. The median value (represented by a horizontal bar) is 6.2, and the standard deviation is 1.2.

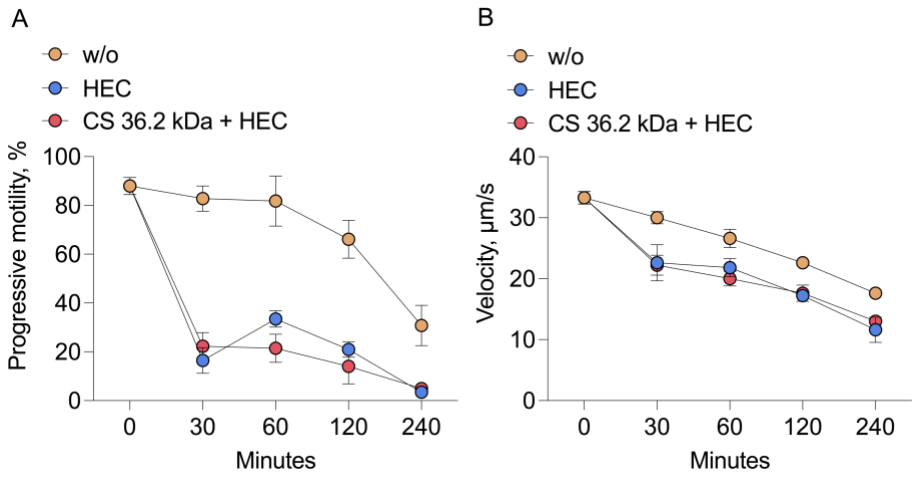

Figure S8. Change in progressive motility and velocity of sperm over time. Semen was either treated with hydroxyethyl cellulose (HEC) or HEC gel with chitosan of 36.3 kDa (CS 36.2 kDa + HEC) and compared to untreated semen (w/o). The time-dependent change in **A**) progressive motility or **B**) velocity over a period of 240 min is demonstrated. Each data point represents the mean of five technical replicates, performed with one semen exhibiting a sperm concentration of 68.48 $\pm$ 5.95 mill/ml and a progressive motility of 87.93 $\pm$ 3.55%. Distribution of values is presented as standard deviation.

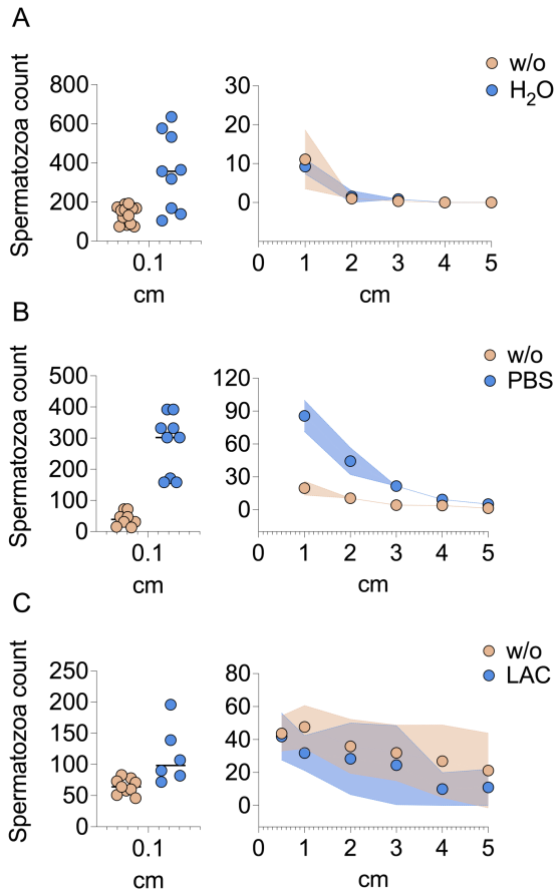

Figure S9. Effect of exposing ovulatory cervical mucus to various solutions on the penetration of sperm. To select for the optimal solution to dissolve chitosan, and to use in sperm penetration tests, we compared the sperm counts at different distances after 30 min exposure of the open end of the capillary filled with cervical mucus (CM) to different solution and then semen for 30 min. Sperm penetration in untreated CM (w/o) is compared to sperm penetration in **A**) water-treated CM (H_2O), in **B**) CM treated with 50 mM phosphate buffered saline (PBS) and in **C**) CM treated with 100 mM lactic acid (LAC). Each measurement was conducted in triplicate, using one or more CM samples. Replicates are the mean of the sperm count at three different fields at each distance. In the left graphs the median is shown. In the right graphs each point is the mean of three measurements, and the colored area represents the standard deviation of the mean.

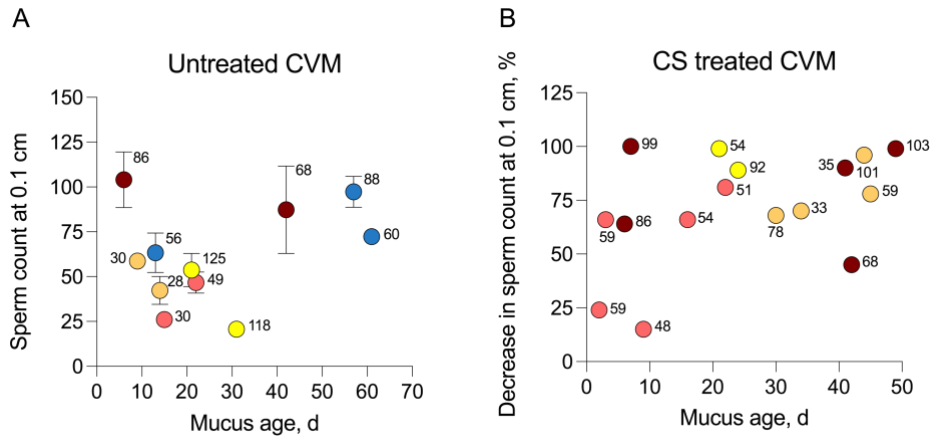

Figure S10. Sperm penetrability is independent on mucus age. A) Semen was exposed to untreated human ovulatory human cervical mucus at 37 °C for 30 min. Sperm numbers were counted at 0.1 cm, the beginning of the capillary. Individual mucus samples are represented with a different color (n = 5). Each mucus sample was three times exposed to semen of the same donor. Nevertheless, the semen differed in sperm count, progressive motility, motility and velocity. We show the variability of sperm concentrations [million sperm/ml] by numbers next to the dots. Means and standard deviations are demonstrated. **B**) Ovulatory human cervical mucus (CM) was treated with chitosan (CS) larger than 7 kDa for 30 min at 37 °C, and the sperm counted at the 0.1 cm of the capillary. The percentage of decrease in sperm number found 0.1 cm into the capillary of CS-treated CM relative to untreated CM was calculated for 16 samples. Each CM sample is shown with a different color. The sperm concentration [million sperm/ml] of the semen used in each experiment is indicated next to each dot.

Tables

Table S1: Characteristics of human semen samples. Values for the days of abstinence of male volunteers before ejaculation, and the characteristics of the semen that was used in in vitro sperm penetration tests. For each of the chitosan oligosaccharide (CO) dissolved in water (H_2O), phosphate buffered saline (PBS) or lactic acid (LAC), and chitosan (CS) dissolved in lactic acid with or without the addition of hydroxyethyl cellulose (HEC), the corresponding semen and its characteristics are presented. Semen viscosity was categorized as unobtrusive (uo.), viscous (vs.) or high viscous (hv.). Distribution of values is presented as standard deviation.

Sample	Abstinence	Volume	Viscosity	Concentration	Progressive	Motile	Immotile	Velocity	Size	Cells
					Spermatozoa					
	d	ml	-	mill/ml	%	%	%	µm/s	µm²	-
CO in H_2O										
	3	1.1	uo.	106.75 ± 6.24	51.61 ± 16.05	62.68 ± 15.59	37.32 ± 15.59	31.45 ± 3.63	14.19 ± 1.28	2208.30 ± 129.17
	5	4.0	uo.	51.09 ± 2.99	58.88 ± 3.52	61.87 ± 3.86	38.13 ± 3.86	21.67 ± 0.50	14.21 ± 0.33	1056.44 ± 61.62
	1	4.2	uo.	37.79 ± 2.56	72.62 ± 3.26	76.40 ± 2.40	23.60 ± 2.40	33.20 ± 1.40	12.34 ± 0.77	781.50 ± 52.90
CO in PBS (semen used twice)	1	2.0	uo.	138.30 ± 9.95	69.30 ± 10.41	78.87 ± 7.39	21.13 ± 7.39	49.10 ± 1.74	15.47 ± 0.64	2860.33 ± 205.51
	3	7.7	uo.	54.96 ± 6.07	80.47 ± 4.66	83.88 ± 3.56	16.12 ± 3.56	29.50 ± 0.53	15.45 ± 1.52	1136.50 ± 125.32
CO in LAC (CS 1.4 kDa)	4	3.0	uo.	44.73 ± 2.33	65.03 ± 5.25	70.14 ± 3.47	29.86 ± 3.47	28.78 ± 1.48	14.08 ± 1.06	925.33 ± 48.56
	2	3.0	uo.	34.92 ± 3.53	50.90 ± 5.46	55.53 ± 5.19	44.47 ± 5.19	27.44 ± 1.88	13.71 ± 0.92	722.78 ± 73.03
	4	2.1	hv.	124.87 ± 5.91	57.69 ± 7.05	65.31 ± 7.11	34.69 ± 7.11	34.20 ± 4.39	13.97 ± 0.78	2483.10 ± 342.24
CS 7.1 kDa										
	3	2.6	uo.	17.28 ± 0.84	51.40 ± 4.13	54.69 ± 5.08	45.31 ± 5.08	30.70 ± 3.71	16.53 ± 0.91	357.20 ± 17.01
	5	3.7	uo.	99.00⁺	68.00⁺	76.00⁺	24.00⁺	-	-	-
	5	2.8	hv.	119.00⁺	71.00⁺	77.00⁺	23.00⁺	-	-	-
CS 18.9 kDa										
	4	3.0	uo.	31.48 ± 6.46	67.56 ± 6.84	70.66 ± 6.34	29.34 ± 6.34	24.89 ± 1.27	12.63 ± 0.87	651.11 ± 133.46
	3	6.9	uo.	59.17 ± 16.30	85.77 ± 7.85	88.30 ± 6.36	11.70 ± 6.36	39.00 ± 2.00	15.68 ± 1.45	1223.90 ± 337.08
	3	5.8	uo.	36.30 ± 5.58	83.58 ± 3.06	85.78 ± 3.19	14.22 ± 3.19	29.90 ± 3.73	18.84 ± 0.93	750.90 ± 115.09
CS 27.9 kDa										
	4	2.0	uo.	103.41 ± 14.21	52.88 ± 17.89	58.15 ± 17.65	41.85 ± 17.65	26.85 ± 4.47	15.15 ± 1.51	2139.10 ± 294.00
	2	2.9	uo.	47.57 ± 3.32	67.62 ± 4.14	72.31 ± 4.06	27.69 ± 4.06	22.20 ± 5.77	14.50 ± 0.88	984.00 ± 68.63
	2	2.2	uo.	59.54 ± 8.45	69.51 ± 6.93	73.77 ± 6.07	26.23 ± 6.07	30.67 ± 2.69	14.67 ± 1.61	1231.78 ± 174.38
CS 35.0 kDa										
	6	6.9	uo.	86.01 ± 6.59	90.68 ± 4.16	92.40 ± 3.24	7.60 ± 3.24	33.60 ± 2.01	14.73 ± 1.44	1778.80 ± 136.40
	3	1.9	uo.	99.43 ± 6.27	89.41 ± 15.90	92.55 ± 10.55	7.45 ± 10.55	37.00 ± 10.09	15.45 ± 1.01	2057.00 ± 129.19

Sample	Abstinence	Volume	Viscosity	Concentration	Progressive	Motile	Immotile	Velocity	Size	Cells
					Spermatozoa					
	d	ml	-	mill/ml	%	%	%	µm/s	µm²	-
	8	3.3	uo.	103.50 ± 7.95	59.86 ± 19.94	68.45 ± 15.76	31.55 ± 15.76	29.07 ± 4.34	13.65 ± 0.75	2141.10 ± 164.19
CS 36.2 kDa										
	3	2.2	uo.	58.71 ± 16.31	88.21 ± 9.38	90.33 ± 7.78	9.67 ± 7.78	34.50 ± 2.88	15.13 ± 0.86	1255.90 ± 284.16
	3	3.1	uo.	53.60 ± 6.62	65.53 ± 8.05	70.78 ± 7.34	25.72 ± 10.39	24.90 ± 8.23	14.51 ± 1.02	1108.80 ± 136.89
	1	1.2	uo.	50.76 ± 1.86	73.21 ± 2.74	76.29 ± 2.70	23.71 ± 2.70	31.60 ± 1.43	14.29 ± 0.65	1050.50 ± 38.17
CS 36.2 kDa desalted										
	4	7.0	uo.	88.35 ± 17.54	90.50 ± 3.75	92.66 ± 2.92	7.34 ± 2.92	29.68 ± 5.21	14.60 ± 0.89	1827.60 ± 362.72
	3	5.1	uo.	32.81 ± 5.02	64.47 ± 7.68	69.01 ± 7.64	30.99 ± 7.64	35.40 ± 1.17	15.01 ± 0.59	671.40 ± 100.70
	3	5.8	uo.	59.60 ± 6.44	94.40 ± 2.31	95.10 ± 2.11	4.90 ± 2.11	44.30 ± 1.64	16.31 ± 0.62	1233.00 ± 133.33
CS 150.0 kDa										
	3	4.5	uo.	32.64 ± 1.97	59.40 ± 5.54	63.10 ± 4.89	36.81 ± 4.87	30.80 ± 0.63	13.65 ± 0.75	674.70 ± 41.14
	4	3.6	uo.	100.93 ± 6.76	93.70 ± 1.84	94.78 ± 1.45	5.22 ± 1.45	33.00 ± 0.47	13.98 ± 0.60	2087.70 ± 140.04
	3	2.0	uo.	58.57 ± 6.57	73.87 ± 7.98	77.42 ± 7.23	22.58 ± 7.23	27.30 ± 0.82	13.98 ± 0.60	1211.70 ± 135.70
CS 290.9 kDa										
	5	3.5	uo.	53.30 ± 4.13	30.73 ± 4.88	37.09 ± 3.86	62.91 ± 3.86	22.90 ± 0.99	15.13 ± 0.86	1102.40 ± 85.57
	4	3.1	uo.	92.06 ± 9.09	81.41 ± 6.73	86.77 ± 2.73	13.23 ± 2.73	23.87 ± 1.04	15.12 ± 1.00	1904.30 ± 187.89
	4	3.1	uo.	85.78 ± 10.54	39.06 ± 1.38	42.90 ± 1.20	57.10 ± 1.20	17.56 ± 2.96	15.76 ± 0.60	1774.20 ± 218.95
CS 1.4 + 35.0 kDa										
	5	3.1	uo.	58.55 ± 5.49	74.50 ± 7.43	77.72 ± 6.69	22.28 ± 6.69	31.30 ± 1.42	13.65 ± 1.27	1211.40 ± 113.78
	2	2.6	uo.	32.60 ± 2.41	49.09 ± 5.77	55.07 ± 5.57	44.93 ± 5.57	28.10 ± 2.18	13.11 ± 0.35	674.50 ± 49.85
	4	2.4	vs.	84.36 ± 5.62	73.70 ± 4.38	78.03 ± 3.12	21.98 ± 3.12	29.38 ± 1.92	13.54 ± 0.80	1745.13 ± 15.87
CS 35 kDa + HEC										
	3	4.0	uo.	34.68 ± 2.50	76.99 ± 4.66	80.69 ± 3.96	19.31 ± 3.96	35.30 ± 1.34	15.12 ± 0.70	717.80 ± 51.59
	3	3.5	uo.	67.87 ± 6.74	89.65 ± 3.19	91.58 ± 2.70	8.42 ± 2.70	33.90 ± 2.38	14.60 ± 1.14	1404.10 ± 139.70
	3	3.0	uo.	70.99 ± 5.74	87.74 ± 1.37	90.01 ± 1.29	9.99 ± 1.29	33.40 ± 1.17	13.43 ± 1.16	1468.70 ± 118.55

+Manually assessed sperm parameters. Computer Aided Semen Analysis system inactive.

Table S2. Collection and characteristics of ovulatory human cervical mucus and hormonal status of female volunteers. Collection and assessment times of the cervical mucus (CM) used in in vitro sperm penetration tests, Insler scoring, volume, and pH, and the follicle stimulating hormone (FSH), luteinizing hormone (LH) and estradiol concentrations in the blood at the time of donation are demonstrated. For each CM, the corresponding chitosan oligosaccharides (CO) dissolved in water (H_2O), phosphate buffered saline (PBS) or lactic acid (LAC), and chitosan (CS) dissolved in lactic acid with or without the addition of hydroxyethyl cellulose (HEC) used in sperm penetration tests are indicated.

CO / CS	Collection	Assessment	Gaping	Quantity	Spinnability	Ferning	Cervix score	Volume	pH	FSH	LH	Estradiol
								µl	-	E/L	E/L	pmol/L
CO in H_2O	06/02/2018	07/02/2018	3	2	2	3	10	983	7.35	20.0	65.0	1004
CO in PBS	26/02/2018	26/02/2018	2	2	3	3	10	954	6.62	8.9	45.0	>2000
CS 7.1 kDa	04/06/2018	04/06/2018	2	2	3	2	9	219	6.70	5.3	14.0	302
CS 7.1 kDa	07/06/2018	07/06/2018[a]	2	1	2	3	8	255	7.01	17.0	60.0	1020
CS 7.1 kDa	18/06/2018	21/08/2018	1	3	1	3	8	566	7.31	4.8	7.4	232
CO in LAC	26/06/2018	26/06/2018	3	3	3	3	12	884	7.29	14.0	51.0	1084
CS 1.4 kDa + 35 kDa												
CS 18.9 kDa	06.12.2018	06.12.2018	3	3	3	3	12	1216	7.31	17.0	44.0	1043
CS 27.9 kDa												
CS 150 kDa	26.03.2019	26.03.2019[b]	3	3	3	3	12	1258	6.51	14.0	47.0	883
CS 18.9 kDa	26.03.2019	27.03.2019	3	3	3	3	12	721	7.07	14.0	52.0	1015
CS 27.9 kDa												
CS 36.2 kDa												
CS 36.2 kDa desalted	26.09.2019	08.10.2019	3	3	3	3	12	841	8.04	11.0	42.0	995
CS 290.9 kDa	28.08.2020	31.08.2020	2	3	3	3	11	919	7.99	7.9	32	1488

[a]CM contained dead sperm. [b]Rod-shaped bacteria observed in CM.

Table S3: Ram semen characteristics (in vitro testing). Two chitosans (CS) were used to analyze the sperm penetration of ram sperm (*n*=2) into ewe ovulatory cervical mucus. The ram sperm cell concentration was calculated by the optical density (OD).

Specimen	Sperm OD	Sperm count [bill/ml]
CS 27.9 kDa	0.25	1.89
	0.32	2.39[+]
	-	1.20
CS 36.2 kDa	0.32	2.39
	0.25	1.89

[+]Kept in milk for 24 h.

Table S4: Sperm count in the ewe reproductive tract. Number of sperms detected in different parts of the reproductive tract after treating ovulating ewes with hydroxyethyl cellulose and chitosan (36.2 kDa) dissolved in lactic acid (32.5 mM, pH 5.5), followed by artificial insemination one hour later. A probe confocal laser endoscope was used to count labeled sperm immediately after artificial insemination (1 h after gel administration) in the vaginal cavity and four hours later (5 h after gel administration) throughout the reproductive tract of ewes. Eight different ewes were used, representing eight individual biological samples. Tests 1-2, 3-5 and 6-8 were conducted on different days.

	Ewe number	**15157**	**20157**	**40105**	**20175**	**14510**	**15336**	**20330**	**40163**
	Experiment	**1**	**2**	**3**	**4**	**5**	**6**	**7**	**8**
1 h	Vagina + Ectocervix	489	502	441	448	664	940	912	1020
5 h	Vagina + Ectocervix	17	141	230	147	209	29	220	997
	Cervix - external os	22	12	83	49	226	35	47	11
	Cervix - internal os	0	0	0	0	4	0	0	0
	Uterus	0	0	0	0	2	0	0	0

Movies

Movie S1
Video clip from the sperm penetration assay performed on human ovulatory CM exposed to 36.2 kDa (Z10) chitosan prior to exposure to sperm. The video is captured 0.1 cm without focusing through the capillary tube. At that distance, the CM is mixed with chitosan that was shown to diffuse clearly over 0.2 cm in the 30 minutes of exposure time. The video shows several sperm with beating flagella, but with no progressive motility.

Movie S2
Video clip from the sperm penetration assay performed on human ovulatory CM exposed to 36.2 kDa (Z10) chitosan prior to exposure to sperm. The video is captured 0.1 cm without focusing through the capillary tube. At that distance, the CM is mixed with chitosan that was shown to diffuse clearly over 0.2 cm in the 30 minutes of exposure time. The video shows several sperm with beating flagella, but with no progressive motility.

Movie S3
Video clip from the sperm penetration assay performed on human ovulatory CM exposed to 35 kDa (95/5) chitosan prior to exposure to sperm. The video is captured 0.1 cm into the capillary tube. At that distance, the CM is mixed with chitosan that was shown to diffuse clearly over 0.2 cm in the 30 minutes of exposure time. The video shows several sperm with beating flagella, but with no progressive motility.

Movie S4
Video clip from the sperm penetration assay performed on human ovulatory CM exposed to 35 kDa (95/5) chitosan prior to exposure to sperm. In this video, the CM was not exposed to chitosan. The video is captured 0.1 cm into the capillary tube. The video shows many sperm actively beating their flagella and with stron